
DEEPTTEST: TESTING AUTONOMOUS DRIVING SYSTEMS WITH REINFORCEMENT LEARNING AND REAL-WORLD WEATHER DATA

A PREPRINT

Chengjie Lu
 Simula Research Laboratory and
 University of Oslo
 Oslo, Norway
 chengjielu@simula.no

Tao Yue
 Simula Research Laboratory
 Oslo, Norway
 tao@simula.no

Man Zhang *
 Kristiania University College
 Oslo, Norway
 man.zhang@kristiania.no

Shaukat Ali
 Simula Research Laboratory and
 Oslo Metropolitan University
 Oslo, Norway
 shaukat@simula.no

ABSTRACT

Autonomous driving systems (ADSs) are capable of sensing the environment and making driving decisions autonomously. These systems are safety-critical, and testing them is one of the important approaches to ensure their safety. However, due to the inherent complexity of ADSs and the high dimensionality of their operating environment, the number of possible test scenarios for ADSs is infinite. Besides, the operating environment of ADSs is dynamic, continuously evolving, and full of uncertainties, which requires a testing approach adaptive to the environment. In addition, existing ADS testing techniques have limited effectiveness in ensuring the realism of test scenarios, especially the realism of weather conditions and their changes over time. Recently, reinforcement learning (RL) has demonstrated great potential in addressing challenging problems, especially those requiring constant adaptations to dynamic environments. To this end, we present *DeepQTest*, a novel ADS testing approach that uses RL to learn environment configurations with a high chance of revealing abnormal ADS behaviors. Specifically, *DeepQTest* employs Deep Q-Learning and adopts three safety and comfort measures to construct the reward functions. To ensure the realism of generated scenarios, *DeepQTest* defines a set of realistic constraints and introduces real-world weather conditions into the simulated environment. We employed three comparison baselines, i.e., random, greedy, and a state-of-the-art RL-based approach *DeepCollision*, for evaluating *DeepQTest* on an industrial-scale ADS. Evaluation results show that *DeepQTest* demonstrated significantly better effectiveness in terms of generating scenarios leading to collisions and ensuring the scenario realism compared with the baselines. In addition, among the three reward functions implemented in *DeepQTest*, *Time-To-Collision* is recommended as the best design according to our study.

Keywords Autonomous driving system testing · Test scenario generation · Reinforcement learning · Software testing

1 Introduction

Autonomous driving systems (ADSs), as cyber-physical systems, sense their operating environment and then autonomously make decisions based on sensed information from the environment. Different from advanced driver-assistance systems (ADASs), which are designed to assist/alert the driver in dealing with dangerous situations, ADSs

*Corresponding author

are designed with the ultimate goal of operating vehicles without human intervention [79]. Testing ADSs has attracted a significant level of attention from both the industry and academia, in recent years. However, testing ADSs is still challenging because of the inherent complexity of ADSs themselves and their operating environment, which is dynamic, high-dimensional, and high-uncertain. In principle, there are an infinite number of driving (and therefore testing) scenarios, and it is critical to ensure that ADSs operate safely under any possible driving scenarios.

Typically, there are two ways of testing ADSs, Offline testing [18] and online testing [36]. Offline testing, also called *model-level* testing, does not test ADSs as a whole but focuses on testing the decision-making deep neural networks (DNNs) by considering DNNs as standalone components without involving the operating environment of ADSs. Several Offline testing approaches [93, 86] have been proposed to test ADSs by generating adversarial test inputs/scenes (e.g., images) for DNNs. Such inputs are typically individual inputs that are expected to find prediction errors of DNNs (e.g., steering angle errors). On the contrary, online testing (or *system-level* testing) aims to identify system-level failures by generating critical test scenarios, in which an ADS under test is deployed in either a simulated or physical operating environment, and the ADS is tested as a whole when it interacts with the environment. Online testing approaches [8, 2, 1, 58] have demonstrated promising performance in identifying system-level failures, but it remains challenging to generate safety-critical test scenarios in a cost-effective way due to the huge time overhead caused by the use of simulated/physical environment.

Existing online testing approaches usually apply techniques such as search algorithms and machine learning. For example, search-based testing (SBT) techniques [8, 2] have been widely used to generate test scenarios by formulating a testing problem (e.g., searching critical configurations of driving scenarios) as an optimization problem, which can be addressed with meta-heuristic optimization algorithms, such as Non-dominated Sorting Genetic Algorithm II (NSGA-II) [23]. However, given the complexity and uncertainty of the ADS operating environment, as well as the complexity of driving decision-making, the application of these approaches are frequently restricted by limited time, cost, and computational resource, or show limited effectiveness in testing a long-term decision-making task under a continuously-changing environment [84]. Recently, reinforcement learning (RL) has shown great potential in addressing various challenging problems, where an agent learns optimal behavior strategies through constantly interacting with its environment without prior knowledge of the environment and the need for labeled training data [47]. Several RL-based testing approaches [58, 20] have been proposed and exhibit good performance in dealing with continuous system and environment status changes. However, such an approach has limited effectiveness in ensuring the realism of test scenarios, especially the realism of weather conditions and their changes over time. Furthermore, there is a lack of empirical studies investigating the effectiveness of different reward functions.

Motivated by the above challenges and the successful applications of RL in solving complicated problems, in this paper, we propose *DeepQTest*, an online ADS testing approach that considers the test scenario generation problem as an environment configuration problem and formulates the sequential interaction between the environment configuration agent and the operating environment as an RL problem. *DeepQTest* configures the operating environment and tests ADSs throughout driving tasks; in each discrete instant of driving in the environment, the RL agent decides an *action* to take on how to configure the environment based on its observation of the environment (*state*), and gets feedback (*reward*) from the environment afterwards. *DeepQTest* adopts *Deep Q-Learning* (DQN) [63], a classical RL algorithm, which has demonstrated excellent performance in addressing various autonomous driving problems, such as lane following [76] and motion planning [16]. To encode the environment states and extract features from the high-dimensional operating environment, *DeepQTest* adopts multi-modal sensor fusion [28] as its state encoding strategy. To ensure the realism of scenarios, we define a set of realistic constraints on configurable parameters (e.g., positions of objects and environmental parameters). We also develop a real-world weather generator that introduces real-world weather data in simulation. Considering the importance of reward functions in RL [46], we carefully design three reward functions: TTC_{Reward} , DTO_{Reward} and $Jerk_{Reward}$, based on three metrics: time to collision (*TTC*), distance to obstacles (*DTO*), and the changing rate of acceleration (*Jerk*). Corresponding to the three reward functions, we design three approaches: $DeepQTest_{TTC}$, $DeepQTest_{DTO}$, and $DeepQTest_{Jerk}$.

We trained 12 *DeepQTest* models using four real-world weather conditions in San Francisco, and the three selected reward functions. The trained models are evaluated with an industrial-level ADS (i.e., Apollo [27]) and a commonly used autonomous driving simulator (i.e., SVL [75]). We perform an extensive empirical study with four driving roads and compare *DeepQTest* with three baseline strategies: random, greedy, and the state-of-the-art approach *DeepCollision* [58]. Evaluation results show that 1) *DeepQTest* outperformed random and greedy strategies in terms of collision generation and time cost for enabling the occurrence of collisions; 2) $DeepQTest_{TTC}$ achieved the overall best performance among all the three reward functions; 3) $DeepQTest_{TTC}$ outperformed *DeepCollision* in terms of generating more realistic collision scenarios with less time, and it also achieved better performance than *DeepCollision* in introducing diverse environment configurations and generating diverse scenarios. Based on the results on the four roads under the four weather conditions with 20 times repetition, *DeepQTest* is able to trigger a realistic collision scenario within 10.57 seconds on average.

The rest of the paper is organized as follows. Section 2 introduces RL, especially the DQN algorithm. Section 3 surveys the existing research on testing ADSs. We present *DeepQTest* in Section 4 and the evaluation design in Section 5. In Section 6, we report results and analyses of the empirical study, followed by discussions in Section 7, and conclude the paper in Section 8.

2 Background

In the section, we provide the required background information about DQN and multi-modal sensor fusion, which are the key techniques applied in *DeepQTest*.

2.1 Deep Q-Learning (DQN)

Reinforcement Learning (RL) is essentially about agents learning decision-making strategies while interacting with environments, which might not be known beforehand. More specifically, during a learning process, based on each observed *state* of the environment, the agent decides an *action* to take, and then the performance of the agent after taking the action is evaluated with a *reward*. The ultimate goal is to maximize the cumulative reward of a long-term decision-making process.

When using Markov Decision Process (MDP) to formulate an RL problem, MDP can be represented as a 5-tuple $\langle \mathcal{S}, \mathcal{A}, \mathcal{R}, \mathcal{P}, \gamma \rangle$, representing a set of states \mathcal{S} , a set of actions \mathcal{A} , a reward function $\mathcal{R}(s_t, a_t)$, a probability distribution $\mathcal{P}(s_{t+1}|s_t, a_t)$, and a discount factor $\gamma \in [0, 1]$. A stochastic policy $\pi : \mathcal{S} \times \mathcal{A} \rightarrow [0, 1]$ maps the state space to a probability distribution over the action space, and $\pi(a_t|s_t)$ represents the probability of choosing action a_t at state s_t . The optimal policy π^* , which represents the goal for an RL agent, is expected to achieve the highest expected cumulative reward: $R_t = \sum_{t>0} \gamma^{t-1} r_t$, where future rewards are discounted by discount factor γ . Discount factor γ controls how an agent regards future rewards; a lower value of γ encourages the agent to focus more on short-term rewards, whereas a higher γ value encourages the agent to be more concentrated on a long-term perspective and maximize long-term rewards. The learning process of an RL agent is that it first observes a state $s_t \in \mathcal{S}$, then based on the observation (i.e., s_t), the agent selects and executes an action $a_t \in \mathcal{A}$. After the execution of a_t , an immediate reward $r_t \sim \mathcal{R}(s_t, a_t)$ is fed back to the agent, along with a newly observed state $s_{t+1} \sim \mathcal{P}(s_{t+1}|s_t, a_t)$.

Many types of RL solutions have been proposed and demonstrate good performance in solving practical problems. One classical method is value-based RL, which uses an action-value function to estimate the performance of an action taken at a given state. Q-learning [91] is a typical value-based method, which employs Q-value as the measure of the expected reward in a state-action pair: (s_t, a_t) . And the action-value function in Q-Learning is called the Q-value function $Q^\pi(s, a) : (\mathcal{S}, \mathcal{A}) \rightarrow \mathbb{R}$, which is the discounted expected return of rewards given the state, action, and policy represented by the equation:

$$Q^\pi(s_t, a_t) = \mathbb{E}_\pi[R_t|s_t, a_t]. \quad (1)$$

The Q-value of a given state-action pair (s_t, a_t) , i.e., $Q^\pi(s_t, a_t)$, is an estimation of the expected future reward obtained from pair (s_t, a_t) with policy π . The optimal action-value function $Q^*(s_t, a_t)$ estimates the Q-value of possible actions for a given state and selects the action with the highest Q-value, based on the Bellman equation:

$$Q^*(s_t, a_t) = \mathbb{E}_{\pi^*}[r_t + \gamma \max_{a_{t+1}} Q^*(s_{t+1}, a_{t+1})]. \quad (2)$$

In Q-Learning, Q-values are stored in a Q-table, which represents the Q-value function for all state-action pairs and updates based on the Bellman function. Such a table is arbitrarily initialized and updated with data representing the agent's experience at each step using the equation:

$$Q(s_t, a_t) \leftarrow Q(s_t, a_t) + \alpha(r_t + \gamma \max_{a_{t+1}} Q(s_{t+1}, a_{t+1}) - Q(s_t, a_t)), \quad (3)$$

where, $0 < \alpha \leq 1$ is the learning rate. A larger learning rate leads to a stronger influence of new data on an update.

One drawback of a Q-table is that when the action space is large and the number of possible states of the environment is infinite, the memory required to store the Q-table, as well as the computation resource required to search from the Q-table, is huge. Therefore, it is very challenging to maintain a separate Q-table for each $\mathcal{S} \times \mathcal{A}$ [15]. Instead, a function is often used to approximate Q-values. To overcome the above challenges, Deep Q-Learning (DQN) [63] was proposed, which approximates and stores Q-values with a neural network (i.e., Q-Network) parameterized by weights

and biases, together denoted as θ : $Q(s, a; \theta) \approx Q^*(s, a)$. DQN employs several mechanisms to ensure the stability of the training process: it first uses a replay memory to store a certain number of state transitions $\langle s_t, a_t, r_t, s_{t+1} \rangle$ and randomly samples data for training the Q-Network. This step aims to reduce correlations among samples and thereby increase sample efficiency through the reuse of data. Second, to ensure the stability of the training process, a separate target network $\hat{Q}(s, a; \theta^-)$ parameterized with θ^- is used for generating target Q-values in Q-Learning updates. \hat{Q} is identical to the main network Q , except that its parameters θ^- are cloned from θ every C update. In this case, the Q-value function is updated as:

$$\theta \leftarrow \theta + \alpha(y_{target} - Q(s_t, a_t; \theta)) \nabla_{\theta} Q(s_t, a_t; \theta), \quad (4)$$

where y_{target} is the target value computed as:

$$y_{target} = r_t + \gamma \max_{a_{t+1}} \hat{Q}(s_{t+1}, a_{t+1}; \theta^-) \quad (5)$$

Finally, at each training iteration, a batch of memory is sampled uniformly from the replay memory for the Q-Network training. The training is based on target Q-values from \hat{Q} . The loss function of Q-Network in DQN is defined as:

$$\mathcal{L}(\theta) = \mathbb{E}[(y_{target} - Q(s_t, a_t; \theta))^2]. \quad (6)$$

2.2 Multi-modal Sensor Fusion

Perception is an essential task of ADSs. To gain robust and reliable environment comprehension, autonomous vehicles are usually equipped with multiple sensors, such as cameras (visual cameras, thermal cameras), LiDARs, and radars [28]. Multi-modal sensor fusion is then a crucial method for perception tasks in autonomous driving. In multi-modal sensor fusion, DNNs are often employed to serve as the environmental perception module by taking a multi-modal representation of a driving environment (high dimensional) as the input and generating a low dimensional feature representation. The input consists of sensor data and vehicle state measurements. As for sensor data, LiDAR point clouds and camera images are often considered. LiDAR point clouds provide both depth and reflectance information of the driving environment and are encoded into different representations such as a bird’s eye view [17] and a front view [54]. Camera RGB images and depth images are also commonly used sensor data to provide rich texture information (e.g., color) of the driving environment. Vehicle state measurements are vehicle dynamics parameters such as speed and acceleration.

By combining LiDAR cloud points, camera images, vehicle measurements, and other sensor data, multi-modal representation can be encoded and inputted into a perception module for feature extraction. To construct a perception module, various neural networks will be adopted. For example, convolutional neural networks (CNNs), which are neural networks with multiple layers, are often used in image or object recognition and classification systems. A typical CNN usually has three types of layers, i.e., convolutional, pooling, and fully connected layers. Convolutional layers are the building block of a CNN, which carry the main computation responsibility, such as identifying edges of images for feature extraction; pooling layers then mitigate the dimensionality of extracted features; fully connected layers, also named output layers, recognize features of an image by using back-propagation algorithms. Due to its exclusive features, such as local connectivity and shared weights, CNN can achieve high accuracy and good performance in various tasks, such as image classification and object detection [22].

Another commonly applied network is the Long Short-Term Memory (LSTM) [39], which is capable of learning long-term dependencies and time series prediction. The key of LSTM is the cell state, which serves as a memory unit where the information can remain unchanged for a sufficient time. This helps the unit to memorize the last calculated value. There are three types of gates in an LSTM memory unit: forget gate, input gate, and output gate, where the forget gate decides which information needs attention and which to ignore, and the input gate updates the memory by controlling the flow of new information into the memory, and the output gate determines the value of the next hidden state, which contains information on previous inputs.

In multi-modal sensor fusion, DNNs represent features hierarchically and offer different schemes to multi-modal sensor fusion, including early, middle, and late fusion schemes. In the early fusion scheme, the multiple representations from raw data are joined together, then the DNN learns the joint features of multiple modalities at an early stage. Early fusion can fully exploit the information of the raw data because data from different sources are directly joined without losing the original information. In the middle fusion scheme, feature representations from different sensing modalities are combined at intermediate layers of a DNN, which enables it to learn cross-modalities with different feature representations. The late fusion scheme uses separate networks for feature extraction of each single sensing

modality (e.g., LiDAR point clouds, camera images), and the outputs are further concatenated and processed by a network to get the final feature representation.

Evidence shows that multi-modal fusion outperforms single-sensor data perception in autonomous driving [28]. Among different fusion schemes, middle fusion has demonstrated promising performance in terms of leading to more accurate object detection [78, 34] and improving the accuracy of geometry and semantics of the resulting representation [71]. Thus, we opt for the middle fusion scheme for multi-modal sensor fusion in our approach.

3 Related Work

As discussed in Section 1, existing ADS testing techniques typically can be classified into *offline* ADS testing (Section 3.1) and online ADS testing (Section 3.2).

3.1 Offline ADS Testing

Offline testing primarily focuses on only testing decision-making DNNs embedded in ADSs without involving an operating environment. There are a large number of offline testing approaches that have been proposed by using machine learning (ML)-based testing [93, 86, 95], fuzz testing [92, 32] and mutation testing [60, 40] techniques to generate adversarial inputs for DNNs in ADSs. To measure test adequacy, various metrics have been proposed, such as neuron coverage [68, 86] and surprise coverage [45].

Several approaches leverage real-world changes in driving conditions (e.g., heavy rain, heavy snow, or adverse lighting), and synthesize adversarial driving conditions using ML techniques. Zhang et al. [93] proposed DeepRoad, an Generative Adversarial Network (GAN)-based unsupervised learning framework, for identifying inconsistent behaviors of DNN-based ADSs under various weather conditions. DeepRoad synthesizes driving scenes with various weather conditions and utilizes metamorphic testing techniques for checking the consistency of such systems under synthetic driving scenes. Tian et al. [86] proposed DeepTest, a systematic testing tool focusing on generating realistic synthetic images by applying image transformations and mimicking different real-world phenomena (e.g., weather conditions, object movements). To explore possibilities for testing ADSs in the physical world, Guo et al. [95] proposed a systematic physical-world adversarial inputs generation approach, named DeepBillboard, which targets a specific driving scenario: drive-by billboards. DeepBillboard generates adversarial perturbations that can be added to roadside billboards in either a simulated/physical world and mislead CNN-based steering models.

Several approaches focusing on deep learning (DL) testing also demonstrate the potential for testing DNNs in ADSs. Guo et al. [32] proposed DLFuzz, a differential fuzzing testing framework, to guide DL systems exposing incorrect behaviors. Xie et al. [92] proposed DeepHunter, a coverage-guided fuzz testing framework, for testing DNNs. DeepHunter detects potential defects of general-purpose DNNs by generating new semantically-preserved test inputs. Ma et al. [60] proposed a mutation testing framework, named DeepMutation, which directly injects faults into DL models through mutation operators. Later on, Hu et al. [40] extended DeepMutation and hence proposed DeepMutation++ to cover more types of DNN models, such as feed-forward neural networks (FNNs) and stateful recurrent neural networks (RNNs).

To measure the test adequacy for DNNs, various metrics [68, 40, 69, 45] for evaluating the test quality have been proposed. For example, Pei et al. [68] proposed DeepXplore, which introduces the neuron coverage for measuring the number of rules in a DNN that have been exercised by a set of inputs, to maximize both the neuron coverage and the number of potentially erroneous behaviors without requiring manual labels. Kim et al. [45] proposed SADL, which introduces surprise adequacy and surprise coverage to measure the test adequacy for DNNs. Such metrics have been applied for guiding the testing of DNNs of ADSs [68, 86] to achieve higher coverages of activated neurons. However, due to an ADS being more complicated than a single DNN model, such DNN testing methods exhibit limitations when being applied to test an ADS with multiple DNN models. Moreover, it has been argued whether metrics such as neuron coverage are meaningful for testing a real-world DNN in ADSs [37].

Offline testing techniques tend to be non-adaptive to contexts where a prediction model needs to adapt to continuous system status changes, which is exactly the case for ADSs' operating environment. This is mainly because such testing techniques test DNNs independent of their ADSs, and based on individual inputs without considering that a single DNN prediction error may have an influence on future predictions and driving decisions [83], leading to system failures. Therefore, although offline testing can detect single prediction errors in DNNs, it shows limitations in identifying system-level failures.

3.2 Online ADS Testing

Online testing approaches have been proposed to test ADSs in a simulated/physical operating environment. Various techniques have been applied in these approaches, including search algorithms and RL.

Search algorithms have been typically applied for generating test scenarios for ADSs and ADASs [1, 2, 11, 8, 12]. These approaches mostly focus on the automated test generation with optimization objectives such as minimizing distances to obstacles or unsafe area [1], maximizing the speed of a vehicle at the time of collision [1], violating safety requirements [2], and minimizing time to collision [11, 8]. Some works apply multi-objective search algorithms to select and/or generate safety-critical scenarios. Abdesslem et al. [8] proposed NSGAI-SM, which combines multi-objective search algorithm NSGA-II [23] with surrogate models [42] to test an ADAS with three objectives. Abdesslem et al. [1] also proposed another approach named NSGAI-DT, which considers two objectives (i.e., speed at the time of collision, distance to obstacles) to generate critical scenarios for vision-based control systems by combining NSGA-II with decision tree classification models. To detect failures caused by feature interactions, FITEST [2] integrates a set of hybrid test objectives designed based on distance functions measuring how far of violating system safety requirements (e.g., no collision with pedestrians, stopping at a stop sign). Such interactions involve features like automated emergency braking (AEB), adaptive cruise control (ACC), and traffic sign recognition (TSR). For instance, a feature interaction may arise when a braking command issued by ABE is overridden by ACC’s command of maintaining the same speed as that of the front vehicle. Calò et al. [12] adapted multi-objective search algorithms (i.e., NSGA-II) to search for collisions and ADS configurations that can avoid such collisions.

While SBT approaches show promising results in supporting online testing of ADSs, they introduce practical challenges in terms of time and computational overhead to evaluate test scenarios [51]. Moreover, another challenge of SBT approaches is that their ability to deal with dynamic and continuously-changing operating environments is limited, which is mainly because they do not take advantage of the interaction between individuals (often encoding test scenarios) with the environment when searching critical scenarios. However, this interaction information has been proven to be efficient for decision-making in RL, especially in an open and dynamic environment under uncertainty [49, 77].

Several RL-based ADS online testing approaches have been proposed [14, 35, 58]. Chen et al. [14] developed an RL-based adaptive testing framework to generate time-sequential adversarial environments specific to lane-changing driving models. Haq et al. [35] proposed MORLOT, an online testing approach, by combining RL and multi-objective search. MORLOT uses RL to adaptively generate sequences of environmental changes that can cause requirement violations and adopts multi-objective search to determine the changes that can cover as many requirements as possible. Lu et al. [58] proposed DeepCollision, an RL-based approach, which generates safety-critical testing scenarios by configuring the operating environment of an ADS. Despite the promising results of the current RL-based approach, there is no work that uses real-world weather data when generating test scenarios. Besides, the literature mainly uses a few parameters to encode RL states, which may have limitations when representing a high dimensional state space of an autonomous driving environment. In addition, designing a proper reward function is vital to an RL-based testing approach, which requires further empirical studies.

To compare with the literature, *DeepQTest*, we propose in this paper, is different from existing RL-based approaches because 1) *DeepQTest* does not try to control the changes of weather conditions, while it introduces real-world weather data to the simulation, which can improve the realism of weather conditions and their changes over time in simulation and therefore improves the realism of test scenarios; 2) *DeepQTest* encodes RL *state* with multi-modal sensor data, which can better represent the environment and system states; and 3) *DeepQTest* integrates three different safety/comfort-related reward functions and evaluates their effectiveness from various perspectives.

4 DeepQTest Methodology

In Section 4.1, we present the overview of *DeepQTest*, followed by a domain model describing all the configurable environment parameters and their relationships. We then describe how we introduce real-world weather data to the simulator (Section 4.3) and mathematically formalize the environment configuration problem as an MDP (Section 4.4). In Section 4.5, we present the preprocessing of sensor data for encoding multimodal states and the Q-network architecture in Section 4.6.

4.1 Overview

DeepQTest learns environment configurations with RL, with the ultimate goal of identifying test scenarios for effectively testing autonomous vehicles, i.e., Autonomous Vehicles Under Test (AVUT). As shown in Figure 1, *DeepQTest* employs a *Simulator* (e.g., LGSVL [75]) to simulate and configure a *Testing Environment*, in which the (virtual) AVUT drives in

its simulated *Operating Environment*. *DeepQTest* also integrates with an *Autonomous Driving System* (e.g., the Baidu Apollo [27]), which is deployed on the AVUT to enable its autonomous driving.

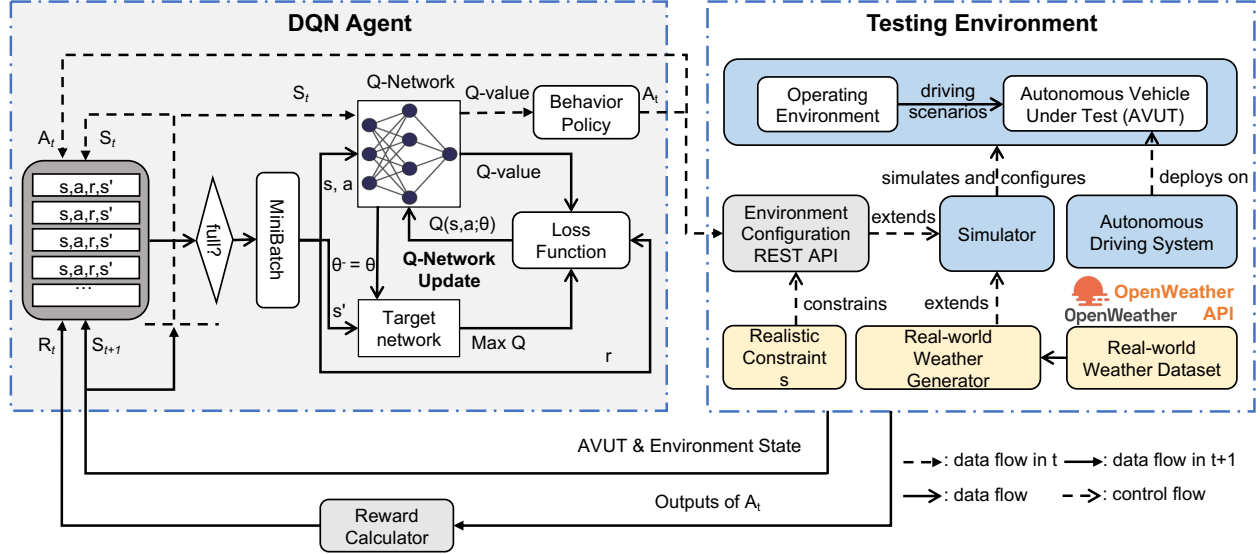


Figure 1: Overview of DeepQTest

DeepQTest utilizes DQN to generate actions to configure the operating environment of the AVUT, e.g., adding a pedestrian crossing the road. As Figure 1 shows, during the configuration process, the DQN agent observes a state S_t describing the current states of the AVUT and its operating environment. With the state, *DeepQTest* decides an action A_t based on the Q-Network and the behavior policy. With our developed *Environment Configuration REST API*, such an action A_t is realized as an HTTP request for accessing the simulator to introduce environment configurations. The realism of the newly configured environment is ensured by *Realistic Constraints* (defined on environment configuration parameters) and *Real-world Weather Generator*, which simulates real-world weather conditions.

After the AVUT drives in the newly configured environment for a fixed time period, i.e., at $t + 1$, both the AVUT and its operating environment enter a new state observed as S_{t+1} , and action A_t produces a set of outputs. Based on these outputs, *Reward Calculator* calculates reward R_t for A_t and S_t at $t + 1$. Then the DQN agent stores them (as $\langle S_t, A_t, R_t, S_{t+1} \rangle$) into the replay memory buffer. Once the replay memory is full, the Q-Network is updated as $Q(s, a; \theta)$, using the loss function by a mini-batch randomly sampled from the updated replay memory. Meanwhile, the target network parameters θ^- are updated with Q-Network parameters θ after a fixed number of steps and remain unchanged between two updates. In addition, with S_{t+1} , the (updated) Q-Network with behavior policy decides the next action: A_{t+1} .

In *DeepQTest*, an episode is finished once the AVUT arrives at its destination, the AVUT cannot move for a defined duration, or a collision happens. At each configuration step, information about the AVUT (e.g., its driving and collision status) and its operating environment (e.g., its status and driving scenarios) are stored as *Environment Configuration Logs* for further analyses and replaying.

4.2 Configurable Environment Parameters

As part of this work, we developed a collection of environment configuration actions as REST API endpoints for manipulating the ADS operating environment by configuring parameters in simulation. These actions are utilized by *DeepQTest* for enabling testing under various operating environment configurations. Figure 2 presents a domain model (in the UML class diagram notations) capturing the *Configurable Parameters* of the operating environment, based on which, *Constraints* can be specified to ensure (to a certain extent) the realism of configured operating environment.

Configurable Parameters. In reality, the operating environment of ADSs constantly changes. However, when testing ADSs in a simulated environment, in practice, the number of parameters that can be manipulated is limited and dependent on the capability of the simulator being used. These configurable parameters and their valid configuration values form the *action space*. Based on the types of objects being configured and properties of effect to create, we classify these parameters into three categories: parameters for configuring *Objects* (*Static Objects*, *Dynamic Objects*), *Road* and *Weather and Time*.

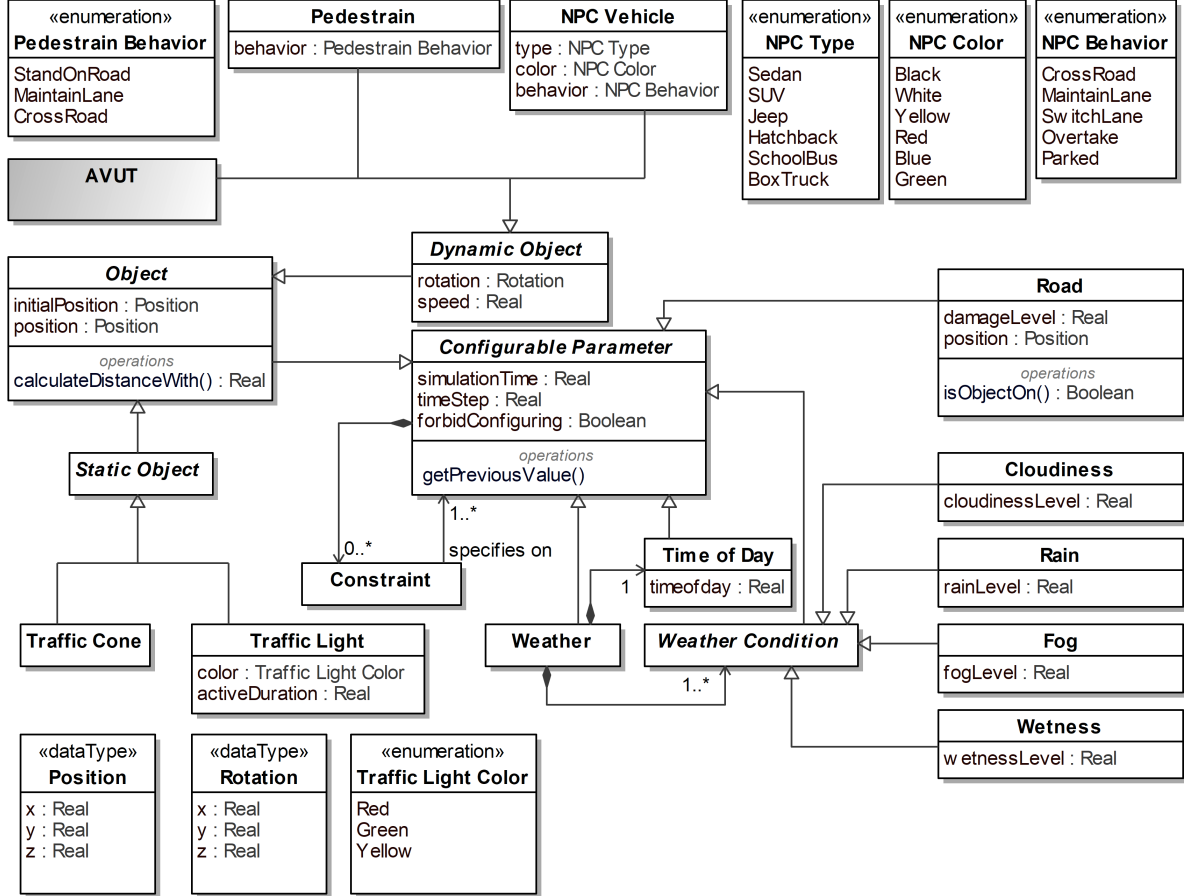


Figure 2: Domain model of the configurable parameters of the ADS operating environment

(1) *Configurable Parameters for Objects.* In the simulated environment, *Object* can be manipulated by configuring its initial position (i.e., *initialPosition* typed with datatype *Position*), retrieving its current position (i.e., *position*), and get a distance with other *Object* with *caclulateDistanceWith*. *initialPosition* can be configured only when the *Object* is introduced into the simulated environment. Such introductions of *Objects* can be performed during testing setup or during testing by an automated testing approach (such as *DeepQTest*). We further classified *Object* into *Static Object* and *Dynamic Object*.

For *Static Objects*, configuration values of the current position (i.e., *position*) remain unchanged within the specified *Simulation Time*. We involve *Traffic Cone* and *Traffic Light* as *Static Objects* in our ADS testing as shown in Figure 2. To test ADS, we allow introducing *Traffic Cone* during testing (e.g., a road accident or a traffic accident could happen when driving), while *Traffic Light* can only be introduced by setup. During testing, configurable parameters of *Traffic Light* include its color (i.e., *color* typed with enumeration *Traffic Light Color*) and duration when the corresponding color is active (*activeDuration* typed with *Real*).

In a simulated environment, *Dynamic Objects* include AVUT, pedestrians and NPC (Non-Player Character) vehicles, and values of their properties (e.g., *position*) change over time as shown by classes *Dynamic Object* (with properties *position* inherited from *Object*, *rotation* and *speed*). AVUT can be configured only in a test setup for a certain objective of testing ADSs, then denoted as grey background. Pedestrians and NPC vehicles can be generated during testing. In addition to the three properties inherited from *Dynamic Object*, a pedestrian has one additional property characterizing itself, i.e., its *behavior* (typed with enumeration *Pedestrian Behavior*). An NPC vehicle has three additional properties: its *behavior* (typed with enumeration *NPC Behavior*), *color* (typed with *NPC Color*), and *type* (typed with enumeration *NPC Type*).

Since pedestrians and NPC vehicles can have a lot of behaviors in real driving environments, the literature mainly focuses on safety-critical behaviors, such as those related to inevitable collisions or traffic rule violations [12, 55]. Such behaviors mainly include overtaking, lane maintenance, lane switching, road crossing, etc. We, consequently,

classify behaviors of pedestrians and NPC vehicles and specify them as two enumerations shown in Figure 2: *Pedestrian Behavior* and *NPC Behavior*.

Realism. To ensure the realism of generations of *Objects*, we defined constraints specified with Object Constraint Language [66] based on the configurable parameters. When introducing a new *Object* into the simulated environment, the *Object* should keep a safe distance from the AVUT and other objects, restricting where the *Object* can be generated with *initialPosition*. Any violation of the safe distance constraint might result in unrealistic scenarios, e.g., colliding with a traffic cone that is just introduced in front of the AVUT, heavy traffic congestion due to generated *NPC Vehicles* which are close to each other. According to Ro et al. [73], a vehicle should keep a safety distance of at least 5 meters from its surrounding objects, however, the volume of *Object* and potential uncertainty in the simulator need to be considered. Then, based on a pilot study, we define the safety distance as 8 meters for *Traffic Cone*, *Pedestrian*, and *NPC Vehicle* with its type of *Sedan*, *SUV*, *Jeep*, and *Hatchback*, and 10 metrics for *NPC Vehicle* with its type of *SchoolBus* and *BoxTruck*. The OCL constraint is defined as:

```
context Object
inv: Object.allInstances → excluding(self) → forAll{o | ((self.oclIsKindOf(TrafficCone)
or self.oclIsKindOf(Pedestrian) or (self.oclIsKindOf(NPCVehicle) and Set{NPCType::
Sedan, NPCType::SUV, NPCType::Jeep, NPCType::Hatchback} → includes(self.asTypeOf(
NPCVehicle).type)) implies self.calculateDistanceWith(o) >= 8) or ((self.
oclIsKindOf(NPCVehicle) and Set{NPCType::SchoolBus, NPCType::BoxTruck} → includes(
self.asTypeOf(NPCVehicle).type)) implies self.calculateDistanceWith(o) >= 10)}
```

For *Traffic Light*, its color changes should also remain realistic. We restrict that the color of traffic lights can be changed only by following the order, i.e., red, green, yellow, then red again. Regarding the active duration for each color, we follow the traffic signal timing manual of the United States Department of Transportation [52], i.e., red 24 seconds, green 30 seconds, and yellow 6 seconds. Then we define the constraint as:

```
context TrafficLight
inv: (self.color =TrafficLightColor::Red implies (self.getPreviousValue().color =
TrafficLightColor::Yellow and self.activeDuration=24)) or (self.color =
TrafficLightColor::Green implies (self.getPreviousValue().color =TrafficLightColor
::Red and self.activeDuration=30)) or (self.color =TrafficLightColor::Yellow
implies (self.getPreviousValue().color =TrafficLightColor::Green and self.
activeDuration=6))
```

(2) *Configurable Parameters for Road.* *Road* can be configured in terms of damage conditions, such conditions would impact ADS that need to be considered in autonomous driving testing [61, 33]. Road damage can be classified into four levels according to Ferlisi et al. [29]: negligible ($damageLevel \in [0\%, 25\%]$), low ($damageLevel \in (25\%, 50\%]$), moderate ($damageLevel \in (50\%, 75\%]$), and severe ($damageLevel \in (75\%, 100\%]$).

Realism. Regarding *Road*, its *damageLevel* cannot be configured (i.e., *forbidConfiguring* is *true*) when AVUT is driving on it. Then, we define a constraint on *Road* as:

```
context Road
inv: (not self.isObjectOn(AVUT)) xor self.forbidConfiguring
```

(3) *Configurable Parameters for Weather and Time.* As shown in Figure 2, *Weather* can be configured with various *Weather Condition* and *Time of Day*. Configuring the time of day has a great impact on illumination conditions such as shadows, direct sunlight, or over/underexposed, which can lead to poor performance of vision-based modules of an ADS [97], thereby important for testing. Similarly, weather conditions are one of the important factors causing accidents for both normal driving and autonomous driving [93, 9]. To test ADSs, we consider four *Weather Conditions*, i.e., *Cloudiness*, *Rain*, *Fog* and *Wetness*, and define different levels for each condition based on real weather dataset as:

- Configuring *Cloudiness* impacts how much the sky in the simulated environment is covered by clouds. To test ADSs with various degree of *Cloudiness*, we defined five levels, i.e., clear sky ($cloudinessLevel \in [0\%, 11\%]$), few clouds ($cloudinessLevel \in (11\%, 25\%]$), scattered clouds ($cloudinessLevel \in (25\%, 51\%]$), broken clouds ($cloudinessLevel \in (51\%, 84\%]$), overcast clouds ($cloudinessLevel \in (84\%, 100\%]$).
- Configuring *Rain* impacts how heavy the rain should fall in the simulated environment. Five levels are defined for *Rain*, i.e., light rain ($rainLevel \in [0\%, 20\%]$), moderate rain ($rainLevel \in (20\%, 40\%]$), heavy intensity rain ($rainLevel \in (40\%, 60\%]$), very heavy rain ($rainLevel \in (60\%, 80\%]$), and extreme rain ($rainLevel \in (80\%, 100\%]$).

- Configuring *Fog* impacts how thick the fog is in the simulated environment. Five levels are defined for *Fog*, i.e., light fog ($fogLevel \in [0\%, 20\%]$), moderate fog ($fogLevel \in (20\%, 40\%]$), heavy fog ($fogLevel \in (40\%, 60\%]$), very heavy fog ($fogLevel \in (60\%, 80\%]$), and extreme heavy fog ($fogLevel \in (80\%, 100\%]$).
- Configuring *Wetness* impacts how much the road in the simulated environment is covered by water in our context. Five levels are defined for *Wetness*, i.e., light wetness ($wetnessLevel \in [0\%, 20\%]$), moderate wetness ($wetnessLevel \in (20\%, 40\%]$), heavy wetness ($wetnessLevel \in (40\%, 60\%]$), very heavy wetness ($wetnessLevel \in (60\%, 80\%]$), and extreme heavy wetness ($wetnessLevel \in (80\%, 100\%]$).

Realism. To ensure the realism of weather and time, in Section 4.3, we design a mechanism that enables to introduce weather conditions based on real-world historical weather dataset with the corresponding time of the day in the simulated environment.

The literature has shown that existing RL techniques cannot handle a large number of discrete actions, which may easily lead to scalability issues [26, 25]. Moreover, since the agent needs to evaluate all possible actions at each step, the larger the *action space*, the larger the training cost (e.g., time) would be. For this reason, we specify valid values of the configurable parameters as enumeration literals, except for the time of day and the speed of any dynamic object, which takes a real value. The overall aim is to reduce the size of the *action space*.

Eventually, invocations of configurable environment parameters are realized via *DeepQTest* APIs we implemented. For this purpose, we implemented in total 142 REST API endpoints [74], which forms the entire *action space* in our current implementation of *DeepQTest*.

4.3 Real-world Weather Generation

As shown in Figure 2, there are various ways of changing weather conditions, such as the time of day, whether it is raining at one moment, and what is the current fog level. In the current design of *DeepQTest*, we decide not to control the change of weather conditions since it is hard to simulate realistic and ever-changing weather conditions. Note that it’s also hard to predict changes in weather conditions over time, even in the real world [80]. Existing works on testing ADSs mainly focus on simulating a fixed weather condition [8, 1] or applying Generative Adversarial Networks (GAN) to generate static weather condition inputs (e.g., GAN-generated images) [93, 86]. These methods, however, cannot generate weather conditions that realistically change over time during a simulation.

Considering the above-mentioned limitations of existing methods, *DeepQTest* directly builds a mapping of weather conditions of the real world to its simulated world. To realize this, we opt for OpenWeather, an open-source online weather database, which provides rich information on history, and current, short-term, and long-term weather forecasts at any location of the globe, and this information can be accessed via APIs.

To map real-world weather conditions to a simulated world, we consider weather data sources from two domains: \mathcal{W}_R , characterized with real-world weather parameters $\{w_r^0, w_r^1, w_r^2, \dots\}$ (e.g., humidity, rain, wind), and \mathcal{W}_S , described with simulated-world weather parameters $\{w_s^0, w_s^1, w_s^2, \dots\}$ (e.g., rain, wetness from a simulator), where \mathcal{R} (or r) and \mathcal{S} (or s) denote the real-world and simulated world, respectively. Given a specific city, since the weather condition in real-world changes over time in a day, we then first map the date and time of day to the corresponding real-world weather condition in the city, $\mathcal{G}_R : (coord; d, t)_R \rightarrow \mathcal{W}_R^{(coord; d, t)_R}$, where $coord$ denotes the coordinates of the given city, d denotes a specific day (in the format of 2021-08-07, for instance), and t specifies the time in a day (e.g., 20:00:00). Given a specific timestamp $(d, t)_R$ of a given city (e.g., San Francisco), the weather condition in real-world can be determined as $\mathcal{W}_R^{(coord; d, t)_R}$. To build a mapping of weather conditions of the real world to its simulated world, we first map the coordinates of the given city in the real world to the simulated world, $\mathcal{M}_{COOR} : coord_R \rightarrow coord_S$. Then, the timestamp $(d, t)_R$ in the real-world is mapped to the simulated world, $\mathcal{M}_T : (d, t)_R \rightarrow (d, t)_S$. Hence, a weather condition of a specific city in the real world with a timestamp $(d, t)_R$ can be mapped as, $\mathcal{M}_{COOR, T} : \mathcal{W}_R^{(coord; d, t)_R} \rightarrow \mathcal{W}_S^{(coord; d, t)_S}$. Thus, with $\mathcal{W}_S^{(coord; d, t)_S}$, we can simulate the weather condition of a specific timestamp of a specific city of the real world in a simulator.

Below we describe how we build \mathcal{G}_R , \mathcal{M}_{COOR} , \mathcal{M}_T and $\mathcal{M}_{COOR, T}$ in detail.

\mathcal{G}_R is built using the OpenWeather APIs. The coordinates $coord$ of a city in the real world are determined by the latitude and longitude of the city: (*latitude, longitude*). The date and time (d, t) is transformed to a Unix timestamp² (e.g., 2021-08-07 20:00:00 is represented as 1628337600 in the Unix timestamp format). Then, with the coordinates $coord$

²The Unix timestamp is a way to track time as a running total of seconds. This count starts at the Unix Epoch on January 1st, 1970 at UTC.

and timestamp (d, t) , we can get access to corresponding weather condition data of the real world via the OpenWeather APIs.

\mathcal{M}_{COORD} and \mathcal{M}_T map the real-world coordinates and timestamp to the simulated world. For \mathcal{M}_{COORD} , *DeepQTest* supports importing High-Definition (HD) maps for testing ADSs in different cities, a HD map contains details including information about coordinates, road shape, and road marking, which are not normally presented on traditional maps [89]. Thus, with the help of HD maps, we can easily map coordinates from the real world to the simulated world. The timestamp mapping \mathcal{M}_T is already supported by the simulator (i.e., LGSVL) itself.

Weather conditions of the real world obtained via the OpenWeather APIs \mathcal{W}_R are characterized by a variety of parameters that can be observed from the real world, including temperature, pressure, humidity, wetness, wind, cloudiness, rain, snow, fog and etc. However, due to the limitations of the simulator we currently use, we can only manipulate 4 types of weather parameters (Figure 2) to simulate weather conditions in the simulated world, which are cloudiness, rain, fog, and wetness. Thus, \mathcal{W}_S is characterized with the parameters below:

$$\mathcal{W}_S = \{w_s^0, w_s^1, w_s^2, w_s^3\} = \{\text{cloudiness}_s, \text{rain}_s, \text{fog}_s, \text{wetness}_s\}$$

Moreover, we select four real-world parameters corresponding to the parameters in the simulator to define \mathcal{W}_R :

$$\mathcal{W}_R = \{w_r^0, w_r^1, w_r^2, w_r^3\} = \{\text{cloudiness}_r, \text{rain}_r, \text{fog}_r, \text{wetness}_r\}$$

Since weather parameters in the real world are described with real values, we correspondingly define real values (shown in Figure 2) for mapping real-world weather conditions to the simulated world. For example, the *cloudiness* level in the real world varies from 0% to 100%. In contrast, in the simulator we use, the *cloudiness* level ranges from 0 to 1, where, 1 is the maximum intensity of *cloudiness*, which is equal to 100% in the real world.

We acknowledge that our current mapping strategy has limitations in terms of not being able to cover a full list of parameters (e.g., *temperature*, *pressure*, *wind*) due to the limitation of the simulator. However, these covered parameters have been proven to be effective in testing ADSs [93, 9]. Moreover, *DeepQTest* can be easily adapted, in future work, to cover more parameters for mapping as long as the simulator being used allows.

4.4 Formulating Environment Configuration Learning as an MDP

4.4.1 State Encoding

In the context of autonomous driving, perception of the driving environment and encoding it to extract features are the key to constructing safety ADSs. In recent years, prior works adopt different approaches to encode the operating environment of an ADS for constructing an object detector [70, 17] or training an end-to-end autonomous driving model [15, 19]. For instance, Codevilla et al. [19] proposed a multi-modal perception method for constructing end-to-end autonomous driving models, and their experiment results indicate that an end-to-end driving model can be improved with multi-modal sensor data (Section 2), instead of just relying on a single modality. To this end, in *DeepQTest*, we adopt multi-modal sensor fusion as the overall strategy of our state encoding. Specifically, a state inputted to the RL model is composed of the following three parts:

- Camera RGB Image: a front view image containing information on the road structure and obstacles ahead;
- Lidar Bird’s Eye View: an eye view representation encoded with height, intensity, and density, containing information of the surrounding environment of the vehicle;
- Vehicle’s State Measurement: measuring the driving state of the vehicle (e.g., speed, acceleration, jerk).

After a state is observed and inputted into the RL model, features will be extracted, based on which the RL agent consequently determines which environment configuration action to take. Details about how a state is processed by the RL model will be presented in Section 4.6.

4.4.2 Action Space

The *action space* in *DeepQTest* is a set of actions with discrete integer values representing the actions’ IDs. These actions are used to configure the driving environment of an ADS, which forms test scenarios for testing the ADS. Each action is associated with a *simulation time* denoted by T (in seconds) and a *time step* denoted by t (in seconds). The *simulation time* T indicates the time we let the simulation run after invoking an action. The *simulation time* is divided into time steps with equal time duration t . Additionally, an action is associated with several outputs, defined as *Environment Configuration Output*.

Outputs of Environment Configuration Actions. In our context, invoking an environment configuration action produces the following three types of outputs.

- *Time-To-Collision (TTC)* measures the time left for a vehicle to collide with obstacles. In our current design of *DeepQTest*, for calculating *TTC*, we adapted the prediction-based method from the Self-Driving Cars Specialization online course [82] provided by the University of Toronto. The pseudocode of the calculation is presented in Algorithm 1.
- *Distance-To-Obstacles (DTO)* measures the distance between AVUT and the obstacles, which is closely related to driving safety [30].
- *JERK* measures the change rate of the acceleration of AVUT, which is one of the important indicators of the degree of comfort of passengers [41].

In *DeepQTest*, values of *TTC*, *DTO* and *JERK* are collected every *time step t*, simultaneously, and after a *simulation time T* of an action being invoked, three lists (TTC_{buff} , DTO_{buff} , $JERK_{buff}$) containing the corresponding outputs are returned.

Algorithm 1 Prediction-Based Time-To-Collision Calculation

Input

Let D be a set of dynamic obstacles; T be time period an environment configuration action will last; dt be time step between simulation steps

Output

A buffer of *TTC* between AVUT with all dynamic obstacles

```

1:  $t \leftarrow 0$ 
2:  $TTC_{buff} \leftarrow []$  ▷ initialize an empty buffer to store TTC
3: while  $t < T$  do
4:    $t = t + dt$ ;
5:    $Pos_{avut}, Velo_{avut} \leftarrow getPosition(avut)$  ▷ get position and velocity of avut
6:   for each  $d \in |D|$  do
7:      $Pos_d, Velo_d \leftarrow getPosition(d)$  ▷ get position and velocity of dynamic obstacle d
8:      $Pos_{coll} \leftarrow collisionPrediction(Pos_{avut}, Velo_{avut}, Pos_d, Velo_d)$  ▷ Predict the collision point between AVUT and d
9:      $TTC_{avut,d} \leftarrow ttcEstimation(Pos_{avut}, Velo_{avut}, Pos_d, Velo_d, Pos_{coll})$  ▷ Estimate time to collision between AVUT and d
10:    Put  $TTC_{avut,d}$  into  $TTC_{buff}$ 
11:   end for
12: end while
13: return  $TTC_{buff}$ 

```

Since *DeepQTest* uses RL with a proper reward function to find test scenarios in a cost-effective manner, we design the reward function based on the outputs of environment configuration actions. Prior works on ADS testing have shown that using *Time-To-Collision*, *Distance-To-Obstacles* as objectives can guide the algorithms to generate safety-critical scenarios [8, 1], and in [6] it is demonstrated that *jerk* is an important factor to passengers' riding experience. We however acknowledge that there might exist other types of outputs, which can be investigated in the future.

4.4.3 Reward Function

The reward function is defined based on the environment configuration outputs (Section 4.4.2). More specifically, to calculate reward, we define three rewards corresponding to the three outputs, denoted as: *Time-To-Collision Reward* (TTC_{Reward}), *Distance-To-Obstacles Reward* (DTO_{Reward}), and *JERK Reward* ($JERK_{Reward}$), respectively.

Time-To-Collision Reward, TTC_{Reward} . A smaller *TTC* indicates a higher collision risk and vice versa [90]. In the context of testing ADSs, we aim to put the AVUT at risk, meaning that smaller *TTC* values lead to higher reward values.

As shown in Algorithm 1, after an environment configuration action is executed, a buffer of *TTC* (i.e., TTC_{buff}) will be returned as an output, and the algorithm then takes the minimum *TTC* in TTC_{buff} for calculating TTC_{Reward} . To apply *TTC* as a metric indicating the risk to collisions, a *TTC* threshold should be determined, denoted as ttc_{thre} , which is configured as 7 seconds, in the current design of *DeepQTest*, based on the guideline from [98]. The calculation of TTC_{Reward} is shown in Equation 7. If a *TTC* value is less than or equal to ttc_{thre} , the reward will be positive; otherwise, a punishment being -1 will be returned.

$$TTC_{Reward} = \begin{cases} -\ln \frac{nor(TTC)}{nor(ttc_{thre})}, & 0 < TTC \leq ttc_{thre} \\ -1, & TTC > ttc_{thre} \end{cases} \quad (7)$$

Distance-To-Obstacles Reward, DTO_{Reward} . Prior works have shown that different distances to obstacles during driving will cause risks of varying severity, and a smaller distance to obstacles will lead to a higher risk of collision, especially when the safety distance is violated [73]. In *DeepQTest*, we take the minimum DTO value from the DTO_{buff} to calculate DTO_{Reward} . The equation for calculating DTO_{Reward} is similar to the calculation of TTC_{Reward} , shown in Equation 8, where, dto_{thre} is the safety distance indicating the minimum distance by which the AVUT avoids a collision with the obstacles. dto_{thre} is related to the kinematics parameters (e.g., speed, acceleration) of the AVUT and obstacles, and in *DeepQTest*, we take the default value from Berkeley algorithm [7] which is 10 meters.

$$DTO_{Reward} = \begin{cases} -\ln \frac{nor(DTO)}{nor(dto_{thre})}, & 0 < DTO \leq dto_{thre} \\ -1, & dto > dto_{thre} \end{cases} \quad (8)$$

JERK Reward, $JERK_{Reward}$. Since the jerk of the AVUT has a strong influence on the comfort of passengers; the higher the jerk, the less comfortable the passengers [6]. When a list of jerks ($JERK_{buff}$) is returned after an environment configuration action is executed, we then take the maximum $JERK$ value in $JERK_{buff}$ for calculating $JERK_{Reward}$. We also need a $JERK$ threshold ($jerk_{thre}$) in the calculation, and according to our preliminary study, we found that for normal driving, the jerk values are lower than $5m/s^3$. Therefore, we set the threshold as $5m/s^3$ since we want to maximize $JERK$.

$$JERK_{Reward} = \begin{cases} \frac{nor(JERK)}{e^{nor(jerk_{thre})}} - 1, & JERK \geq jerk_{thre} \\ -1, & 0 \leq JERK < jerk_{thre} \end{cases} \quad (9)$$

Considering that environment configuration outputs (TTC , DTO , and $JERK$) may be not comparable, in the above calculations, we apply the normalization function [31], $nor(F_x) = (F_x - F_{min}) / (F_{max} - F_{min})$, to ensure all values fall into $[0, 1]$, where, F_x is an environment configuration output to be normalized; max and min represent the maximum value and minimum value of the environment configuration output, respectively.

4.5 Sensor Data Preprocessing

Some preprocessing steps for camera images and lidar point cloud data in multimodal state encoding are necessary because working directly with raw data can be computation and memory demanding [63]. In *DeepQTest*, a camera image is an RGB image of 1920×1080 pixel frames at each color channel, we crop off the top rectangle area of the image so that the picture in front of the vehicle is centered in the image, then resize the cropped image to 160×376 pixel frames at each color channel while keeping its aspect ratio constant.

A lidar sensor generates a point cloud P containing N points: $P = \{p_1, p_2, \dots, p_N\}$, $p_i = (x, y, z, r)^T$, $i \in \{1, 2, \dots, N\}$, where (x, y, z) denotes a 3D position in space and r denotes the reflectance of point p_i . To get a bird's eye view representation from the point cloud, we follow the steps from MV3D [17] to encode a bird's eye view representation with height, intensity, and density. Hence, the point cloud is discretized into a 2D grid with a resolution of 0.1 meters. The height of each cell in the grid is calculated as the maximum height of the points. The intensity is the reflectance value of the maximum height point. The density is computed using the number of the points in the cell (n) as $\min(1.0, \frac{\log(n+1)}{\log(64)})$. To encode more detailed height information, the point cloud is divided equally into M slices.

Finally, the bird's eye view is encoded as $(M + 2)$ -channel features. In *DeepQTest*, we are using a lidar sensor with 128 laser beams, which can generate 9391 points in one point cloud. Thus, in total the bird's eye view is a 15-channel feature with size 300×300 at each channel.

4.6 Network Architecture and Training Algorithm

4.6.1 Network Architecture

Deep Q-Learning (Section 2.1) utilizes a neural network (Deep Q-Network) to approximate and store Q-values and the design of the Q-Network plays a key role in learning tasks. In the context of autonomous driving, a good network architecture is conducive to the learning tasks, such as the success in image classification (e.g., VGGNet [81], Alexnet [53]), object detection (e.g., MV3D [17]) and pedestrian prediction [44]. Focusing on multimodality and sensor data fusion, various network architectures have been proposed as well as various fusion schemes. As discussed in Section 2.2, the middle fusion scheme has demonstrated promising performance in various autonomous driving perception tasks, which gives us the confidence to adopt the middle fusion scheme to construct the Q-network in *DeepQTest*.

Assume that each state $s = \langle \mathbf{i}, \mathbf{b}, \mathbf{m} \rangle$ comprises an image \mathbf{i} , a lidar bird’s eye view \mathbf{b} , and a low-dimensional vector \mathbf{m} referring to vehicle state measurements. The deep neural network (DNN) in a DQN algorithm takes a state as the input and produces an action with the maximum Q-value as its output. As shown in Figure 3, the network includes an image-processing CNN module, taking image \mathbf{i} as the input to extract image features $C(\mathbf{i})$; a lidar-processing CNN module which takes lidar bird’s eye view \mathbf{b} as the input to extract lidar bird’s eye view features, $C(\mathbf{b})$; and a module of fully-connected neural network (FNN) which takes vehicle state measurements as the input to extract measurement features, $F(\mathbf{m})$. After a state is processed by these three modules, the output features (i.e., $C(\mathbf{i})$, $C(\mathbf{b})$, $F(\mathbf{m})$) are concatenated into a joint representation:

$$j = J(i, b, m) = \langle C(i), C(b), F(m) \rangle \quad (10)$$

The final decision module, implemented as an LSTM [39], followed by two fully-connected layers, takes the joint representation \mathbf{j} as input and outputs an action with the maximum Q-value.

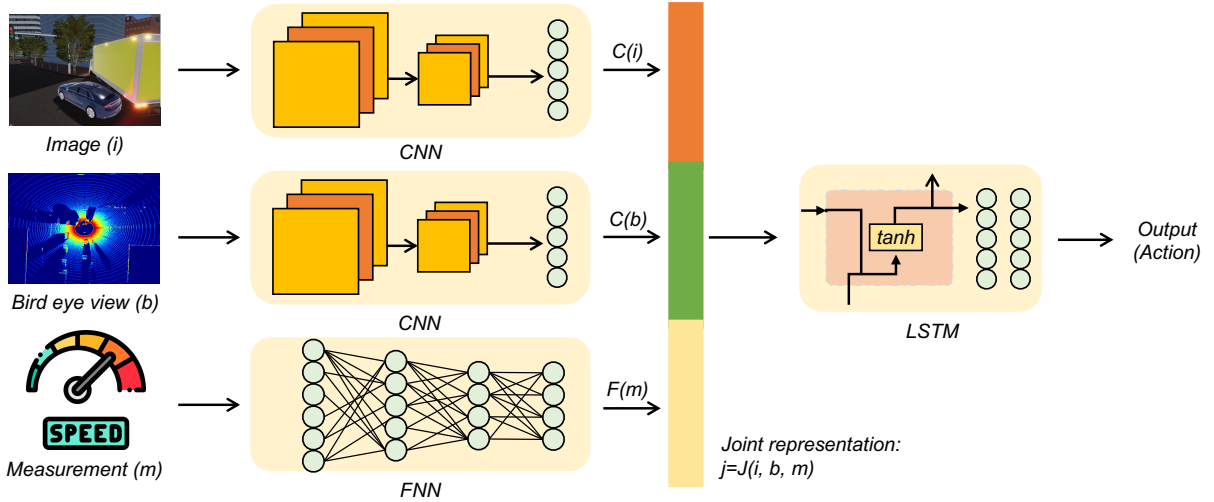


Figure 3: **Q-Network Architecture.** The RGB image, bird’s eye view, and vehicle status measurement are the inputs of Q-Network. The output is the environment configuration action.

More specifically, the image-processing CNN module consists of 4 convolutional layers and 2 fully-connected layers. The input \mathbf{i} consists of a $160 \times 376 \times 3$ image. The first hidden layer convolves 32 filters of 5×5 with stride 4. The second hidden layer convolves 64 filters of 3×3 with stride 2. The third hidden layer convolves 128 filters of 3×3 with stride 2, followed by the final convolutional layer that convolves 256 filters of 3×3 with stride 2. This is followed by a hidden and fully-connected layer with its neuron number (128 neurons) equal to the output of the last convolutional layer of the module. The lidar-processing CNN module has the same design as the image-processing CNN module, but with its input \mathbf{b} being a $300 \times 300 \times 15$ image. The FNN module with its input as measurement \mathbf{m} is designed as a four-layer fully-connected neural network with the architecture of an input layer with 1 neuron, 200 hidden layers with 200 neurons for each, and one output layer with 64 neurons. The final decision module consists of an LSTM with 704 neurons as the input, 64 hidden neurons, and 2 recurrent layers, which is followed by a fully-connected hidden layer with 64 neurons and another fully-connected layer for outputting an action with the maximum Q-value. To ensure stability, prevent overfitting, and accelerate the convergence of the network training process, we perform

Table 1: Description of tasks, employed approaches, road settings, weather condition settings, metrics, and statistical test for each RQ

RQs	Tasks	Approaches	Roads	Weather	Metrics (Section 5.4)	Statistical Test
RQ1	Compare <i>DeepQTest</i> with <i>RS</i> and <i>GS</i>	<i>DeepQTest</i> <i>RS, GS</i>			<i>Safety and Comfort Metrics</i>	Mann-Whitney U test Vargha-Delaney A measure
RQ2	Identify the best reward function of <i>DeepQTest</i>	<i>DeepQTest_{TTC}</i> <i>DeepQTest_{DTO}</i> <i>DeepQTest_{Jerk}</i>	<i>R1</i> <i>R2</i> <i>R3</i> <i>R4</i>	<i>Rainy Day</i> <i>Rainy Night</i> <i>Sunny Day</i> <i>Rainy Day</i>	<i>Safety and Comfort Metrics</i> <i>Diversity Metrics</i>	Mann-Whitney U test Vargha-Delaney A measure Spearman’s rank correlation coefficient
RQ3	Compare <i>DeepQTest</i> with the state-of-the-art in terms of the effectiveness of detecting unrealistic collision scenarios, and the diversity of generated scenarios.	<i>DeepQTest_{TTC}</i> <i>DeepCollision</i>			<i>Realism Metrics</i> <i>Diversity Metrics</i>	Mann-Whitney U test Vargha-Delaney A measure

batch normalization after each convolutional layer, then apply the Rectified Linear Unit (ReLU) nonlinearity after each normalization. We also apply the ReLU nonlinearity after each fully-connected layer and use 10% dropout after LSTM.

5 Experiment Design

5.1 Research Questions

To assess our approach, we carried out an empirical study to answer the following three main research questions (RQs):

RQ1: Does *DeepQTest* achieve better performance compared to *Random* and *Greedy Strategies*? RQ1 aims to do a sanity check that the problem we address is complex and it is hard to be solved by naive *Random* and *Greedy Strategies*.

RQ2: Among the three reward functions, which one performs the best? RQ2 aims to identify the best design(s) (Section 4.4.3), which can guide *DeepQTest* to generate more effective environment configurations for testing AVUT.

RQ3: How does the *DeepQTest* perform compared to the start-of-the-art technique? RQ3 aims to demonstrate the effectiveness of *DeepQTest* compared to the start-of-the-art technique, i.e., *DeepCollision*.

Table 1 shows an overview of our experiment design. In the rest of this section, we present comparison baselines (Section 5.2), experiment settings (Section 5.3), evaluation metrics (Section 5.4), and statistical test (Section 5.5).

5.2 Comparison Baselines

To evaluate *DeepQTest*, we selected three baseline techniques, i.e., a random strategy (i.e., *RS*), a greedy strategy (i.e., *GS*), and *DeepCollision* [58]. *RS* is commonly used as the baseline for a sanity check on whether an optimization problem is complex enough. *GS* has been used as the comparison baseline in the literature for several RL-based approaches, including RL-based decision-making for autonomous lane changing [64] and RL-based navigation optimization [3]. *DeepCollision* is a recent study that is an RL-based ADS testing strategy proposed by Lu [58] for testing AVUT with various environment configurations. Detailed implementations and setup for each baseline are:

1. **RS** (Algorithm 2): *RS* randomly selects an action to configure the environment at each environment configuration step.
2. **GS** (Algorithm 3): *GS* was implemented to select the best configuration at each step. To determine the next action to be executed, *GS* executes all the actions (Lines 7–14), then selects an action that achieves the best performance based on a defined reward (Line 15). For *GS*, we implemented three rewards as *DeepQTest* (i.e., *TTC*, *DTO*, and *Jerk*), and comparison was conducted by employing the same reward (e.g., *DeepQTest_{TTC}* vs. *GS_{TTC}*). To ensure that the comparison among actions is fair, we implemented a *rollback* mechanism (see Line 13) that facilitates, at each iteration, executing each action from the same state of the testing environment. A sequence of the best actions is returned at the end of the search.
3. **DeepCollision** [58]: *DeepCollision* learns environment configurations with RL guided by the collision probability to maximize collision occurrences. There are four models trained in *DeepCollision*, and we selected the recommended one [58], i.e., *M6* model, in our experiment. In *DeepCollision*, a state of the driving environment is encoded based on 8 environmental parameters, while *DeepQTest* adopts multi-modal sensor fusion to encode the state. Compared to *DeepCollision*, we further consider realism by defining realistic constraints in *DeepQTest* to ensure that AVUT can be tested with realistic scenarios. To better explore testing of ADS with various environment configurations, in *DeepQTest*, we involved 90 more environment configurations APIs than *DeepCollision*, i.e., 142 APIs in *DeepQTest* vs. 52 APIs in *DeepCollision*.

Algorithm 2 RS-based Environment Configuration**Input**

Let $TEnv$ be the test environment; AS be the environment configuration action space; $terminate$ be the stopping criteria.

Output

Act_{list} : a list of actions selected from AS

```

1:  $Act_{list} \leftarrow []$ 
2:  $s \leftarrow$  observe a state from  $TEnv$ 
3: while  $\neg terminate$  do
4:    $act \leftarrow$  randomly select an action from  $AS$ 
5:    $terminate, reward, s' \leftarrow$  step( $act, s$ ) ▷ execute the selected action in state  $s$ 
6:   Put  $act$  into  $Act_{list}$ 
7:    $s \leftarrow s'$ 
8: end while
9: return  $Act_{list}$ 

```

Algorithm 3 GS-based Environment Configuration**Input**

Let $TEnv$ be the test environment; AS be the environment configuration action space; $terminate$ be the stopping criteria.

Output

Act_{list} : a list of actions selected from AS

```

1:  $Act_{list} \leftarrow []$ 
2:  $s \leftarrow$  observe a state of  $TEnv$ 
3:  $TEnv_{pre} \leftarrow$  SaveEnv( $TEnv, s$ ) ▷ save the  $TEnv$  with state  $s$ 
4: while  $\neg terminate$  do
5:    $reward_{max} \leftarrow 0$ 
6:    $act_{optimal} \leftarrow 0$ 
7:   for each action  $act$  in  $AS$  do ▷ try each action in the action space
8:      $_, reward, _ \leftarrow$  step( $act, s$ )
9:     if  $reward > reward_{max}$  then
10:       $reward_{max} \leftarrow reward$ 
11:       $act_{optimal} \leftarrow act$ 
12:     end if
13:    $TEnv \leftarrow$  RollBackEnv( $TEnv_{pre}, s$ )
14: end for
15:  $terminate, reward, s' \leftarrow$  step( $act_{optimal}$ ) ▷ execute the action that achieves the maximum reward
16: Put  $act_{optimal}$  into  $Act_{list}$ 
17:  $TEnv_{pre} \leftarrow$  SaveEnv( $TEnv, s'$ )
18:  $s \leftarrow s'$  ▷ move to the next environment state
19: end while
20: return  $Act_{list}$ 

```

5.3 Experiment Settings

5.3.1 Subject System and Simulator

To evaluate *DeepQTest*, we adopt Baidu’s open-source autonomous driving platform Apollo [85] as the subject system under test, which is a high-performance ADS with various modules responsible for various tasks, such as traffic light recognition, obstacle perception and avoidance, and trajectory planning and routing. Apollo is a flexible architecture with high-driving automation, aiming to support the development, testing, and deployment of autonomous vehicles. Concretely, we used the Apollo Open Platform 5.0, which can operate without human interactions in most circumstances and handle complex road scenarios with enhanced perception deep learning models.

We adopt LGSVL Simulator [75] to simulate the autonomous vehicle and its operating environment. Specifically, LGSVL is an open-source, high-fidelity autonomous driving simulation platform that provides an essential vehicle dynamic model for vehicle simulation and supports a set of sensors, including cameras, LiDAR, GPS, and Radar. LGSVL can easily connect to autopilot platforms such as Apollo and Autoware [43], enabling us to perform software-in-the-loop and hardware-in-the-loop ADS testing. In our experiment, we employed LGSVL Simulator 5.0. We selected the San Francisco HD map, a digital re-creation of a section of the South of Market Street (SoMa) in San Francisco

with various driving environment characteristics, e.g., traffic light intersections and multi-lane streets. Regarding the AVUT, we used Lincoln2017MKZ, a four-door Sedan car equipped with various sensor configurations.

5.3.2 Model Training

We selected 4 different types of real-world weather conditions (shown in Table 2) in San Francisco from the OpenWeather dataset. Next, we trained 12 (3 reward settings \times 4 real-world weather conditions) *DeepQTest* models. Accordingly, we defined 12 *RS* and 12 *GS* strategies. We use convention $DeepQTest_{[reward][real-world-weather]}$ to denote each trained model, and use $GS_{[reward][real-world-weather]}$, $RS_{[reward][real-world-weather]}$ to denote each baseline strategy (Section 5.2). For example, $DeepQTest_{TTC_{RD}}$ denotes the model trained in the rainy day (RD) with reward function TTC_{Reward} .

All models were trained with the same network architecture, learning algorithm, reward design, and hyperparameter settings to ensure fair comparisons. For training each model, we used the Adam algorithm [94] with mini-batches of size 64 as the adaptive optimization algorithm. To manage the trade-off between exploration and exploitation, we applied ϵ -greedy as the behavior policy during training with ϵ annealed from 1.0 to 0.2 over the first 10000 observed states and fixed at 0.2 thereafter. Such a setting of behavior policy lets the agent explore more at the beginning of the training process when little is known about the problem environment, and as the training progresses, the agent gradually conducts more exploitation than exploration. We trained for a total of 40000 observed states and used a replay memory with a size of 6000.

Table 2: Real-world weather conditions applied in the experiment

	Rainy Day (RD)	Rainy Night (RN)	Sunny Day (SD)	Sunny Night (SN)
Date	2021-08-07	2021-08-07	2021-07-24	2021-07-24
Time	8:00:00	20:00:00	8:00:00	20:00:00
Description	Heavy intensity rain	Heavy intensity rain	Clear sky	Clear sky

Based on our pilot study, we found that directly training on a huge HD map with many roads is not easy. Because we are trying to generate complex driving scenarios for an AVUT driving from origin to destination, thus if the driving path is too long, then it will take much more time for one episode. Moreover, as the training progresses, the environment will be more complex for the AVUT arriving at the destination, therefore, collisions tend to occur early in the driving task. Thus, we divided the map into road segments with lengths of about 1km to 2km. Next, we trained each model on each road segment to gain a final model. This allows the agent to finish one episode within a reasonable time and ensures that the whole road is fully explored and exploited.

The values of all hyperparameters are determined based on the parameter settings from [63, 67]. We provide the settings of all hyperparameters in our online repository (see Section 6.5).

5.3.3 Experiment Design and Execution

Roads. To ensure that the experiments are run in the same environment, we used the same roads adopted in *DeepCollision* [58], which are selected based on the road structure definition in [21]. Figure 4 graphically depicts their characteristics.

Driving Scenarios. A driving scenario S describes the temporal development between several scenes, where a scene describes a snapshot of the environment including the AVUT, static and dynamic obstacles, and environmental conditions such as weather and traffic rules [87]. We, therefore, formally define a driving scenario as a tuple with scenes: $S = \langle scene^1, scene^2, \dots, scene^n, ST \rangle$, where ST is the time period that the scenario spans and n denotes the number of scenes in the scenario. A driving scene is a 3-tuple $\langle AVUT\ Operation, AVUT\ Speed, Environment\ State \rangle$, denoting AVUT operations such as cruise, a speed level of the AVUT, e.g., zero or slow, and 3) environment state about weather condition, time of date, traffic rules, obstacles, and their behaviors, etc. More specifically, we use 11 properties (column 3, Table 3) to characterize AVUT’s states (rows 1 and 2, Table 3) and the environment (rows 3 to 11, Table 3). Note that NPC vehicles, Pedestrians, Static obstacles, Traffic Lights, and Sidewalks are collected within the sensing range of the radar deployed on the AVUT. Moreover, in our current design, the time period that the scenario spans (i.e., ST) is set to 3 seconds.

Execution. To answer the RQs (Section 5.1), each trained *DeepQTest* model, *RS*, *GS*, and *DeepCollision* were run 20 times on each of the four roads (R1...R4). The trained *DeepQTest* models were evaluated with an ϵ -greedy behavior

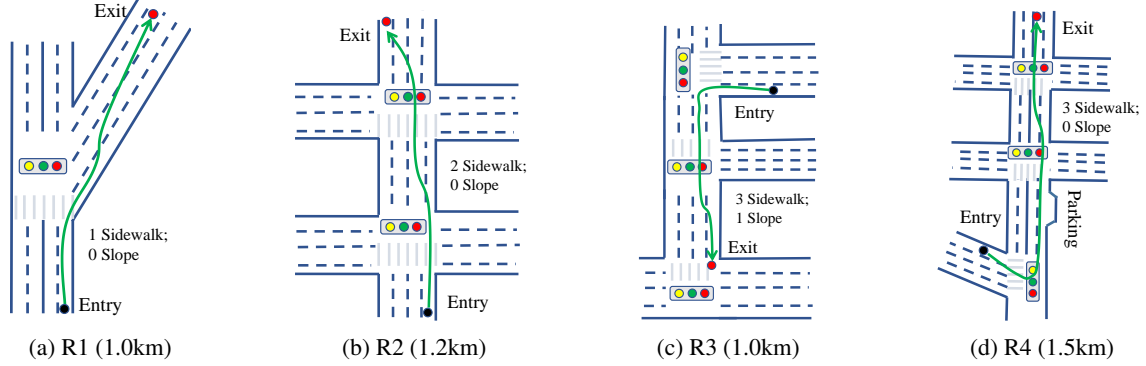


Figure 4: Graphical representations of the roads from [58]

Table 3: Properties characterizing scenes in the formal experiment

#	Property	Property Value
1	AVUT	Operation Stop; Cruise; SpeedUp; SpeedCut; EmergencyBrake; SwitchLaneToRight; SwitchLaneToLeft; TurnLeft; TurnRight
2		Speed (m/s) Zero ($0 < \text{speed} \leq 1$); Slow ($1 < \text{speed} \leq 5$); Moderate ($5 < \text{speed} \leq 12$); Fast ($\text{speed} > 12$)
3	Weather: rain	None ($\text{rain}_{\text{level}} = 0$); Light ($0 < \text{rain}_{\text{level}} \leq 0.2$); Moderate ($0.2 < \text{rain}_{\text{level}} \leq 0.5$); Heavy ($\text{rain}_{\text{level}} > 0.5$)
4	Weather: fog	None ($\text{fog}_{\text{level}} = 0$); Light ($0 < \text{fog}_{\text{level}} \leq 0.2$); Moderate ($0.2 < \text{fog}_{\text{level}} \leq 0.5$); Heavy ($\text{fog}_{\text{level}} > 0.5$)
5	Weather: wetness	None ($\text{wetness}_{\text{level}} = 0$); Light ($0 < \text{wetness}_{\text{level}} \leq 0.2$); Moderate ($0.2 < \text{wetness}_{\text{level}} \leq 0.5$); Heavy ($\text{wetness}_{\text{level}} > 0.5$)
6	Time of the day	Morning (10am); Noon (12am); Night (8pm)
7	Env	<i>Volume</i> (m^3): Small ($\text{volume} \leq 10$); Medium ($10 < \text{volume} \leq 60$); Large ($\text{volume} > 60$)
8		<i>Operation</i> : Stop; SwitchLane; LeftLaneDriving; RightLaneDriving; CurrentLaneDriving
9	NPC vehicle*	<i>Speed</i> (m/s): Zero ($0 < \text{speed} \leq 1$); Slow ($1 < \text{speed} \leq 5$); Moderate ($5 < \text{Speed} \leq 12$); Fast ($\text{speed} > 12$)
10		<i>Distance from AVUT</i> (m): Zero ($ d = 0$); Very near ($0 < d \leq 8$); Near ($8 < d \leq 18$); Far ($18 < d \leq 28$); Very far ($ d > 28$)
11	Pedestrian*	<i>Volume</i> (m^3): Small ($\text{volume} < 1$)
12		<i>Operation</i> : Stop; Crossing the road; FrontLaneWalking
13	Static obstacles*	<i>Distance from AVUT</i> (m): Zero ($ d = 0$); Very near ($0 < d \leq 8$); Near ($8 < d \leq 18$); Far ($18 < d \leq 28$); Very far ($ d > 28$)
14		<i>Volume</i> (m^3): Small ($\text{volume} \leq 3$); Medium ($3 < \text{volume} \leq 10$); Large ($\text{volume} > 10$)
15	Traffic Rule: traffic light	None; Green (allow to pass but slow at intersection); Yellow (stop for a while); Red (do not run a red light)
16	Traffic Rule: side walk	None; SlowDown

policy with $\epsilon=0.05$. As suggested by Mnih [63], this setting is adopted to minimize the possibility of overfitting during evaluation. In total, we obtained results of 2880 executions (20 runs \times 4 roads \times 3 strategies \times 3 reward functions \times 4 Real-World Effects). All the experiments were executed on three machines with identical configurations with a 2.4GHz Intel Xeon E5-2680 v4 CPU, an 11GB NVIDIA GeForce GTX 1080 Ti GPU, and 32GB RAM. The operating systems are all Ubuntu 18.04.6 LTS.

5.4 Evaluation Metrics

In this section, we present the definition of the evaluation metrics: *Safety and Comfort Metrics*, *Realism Metrics*, and *Diversity Metrics*. As shown in Table 1, for RQ1, we use *Safety and Comfort Metrics* to evaluate the performance of *DeepQTest* when comparing with *RS* and *GS*. We adopt *Safety and Comfort Metrics*, and *Diversity Metrics* to evaluate the performance of the three reward functions of *DeepQTest* (RQ2). Regarding the comparison with *DeepCollision* (RQ3), we use *Realism Metrics* to evaluate the realism of the generated scenarios because both *DeepQTest* and *DeepCollision* have different mechanisms to ensure the scenario realism, and *Diversity Metrics* is used for evaluating the diversity of environment configurations and scenarios of the two approaches.

5.4.1 Safety and Comfort Metrics

In *DeepQTest*, we defined three reward functions based on *TTC*, *DTO*, and *Jerk*, respectively, which are related to driving safety or comfort. In our evaluation, we employed them to study the performance of the reward functions and their potential correlations. These metrics are formally defined as Equation 11, where k denotes the k th execution, and i denotes the i th simulation time T (see Section 4.4.2) in the execution.

$$SCM_k = \frac{\sum_{i=1}^n SCM_k^i}{n}, SCM \in \{TTC, DTO, Jerk\}, k = 1 \dots 20 \quad (11)$$

In addition, during each execution k , we collected the number of collisions $\#Collision_k$. $\#Collision_k$ could be 0 if no collision occurred. For *DeepQTest*, $\#Collision_k \in \{0, 1\}$ as it terminates the execution once a collision is identified. For *DeepCollision*, $\#Collision_k$ could be more than one, because *DeepCollision* allows the AVUT to continue to move forward after the occurrence of a collision. We also calculated $CollisionTime_k$, which measures how long a collision can be observed on average.

5.4.2 Realism Metrics

To evaluate *DeepQTest* and *DeepCollision* in terms of whether they generate realistic scenarios, in addition to the *realistic constraints on Objects and Roads* (Section 4.2), we further define a set of *realistic constraints* on the parameters for weather and time. Specifically, for weather and its change over time, we ensure its realism based on four weather-related measurements which can be observed in the simulator, i.e., rain, cloudiness, fog, and wetness. By analyzing real-world historical weather data from an open weather dataset, i.e., OpenWeather³, we calculate the range of realistic changes over time of these four weather-related measurements and then define the following constraints for ensuring the realism of the weather and its change.

- *Rain* reflects the intensity of the rainfall, to be realistic, the rain level change within 1 hour should be less than 20%.

```
context Rain
inv: self.rainLevel <= (self.getPreviousValue(1h).rainLevel+0.2).max(1.0) and
    self.rainLevel >= (self.getPreviousValue(1h).rainLevel-0.2).min(0.0)
```

- *Cloudiness* refers to the extent to which the atmosphere is covered by clouds (measured by *cloudinessLevel* in Figure 2). For instance, cloudiness which is less than 30% represents a clear sky while near 100% cloudiness represents an overcast sky. To be realistic, the cloudiness level change within an hour should be less than 25%. For example, if the current cloudiness is 25%, the realistic cloudiness within one hour should be between 0% and 50%.

```
context Cloudiness
inv: self.cloudinessLevel <= (self.getPreviousValue(1h).cloudinessLevel+0.25).
    max(1.0) and self.cloudinessLevel >= (self.getPreviousValue(1h).
    cloudinessLevel-0.25).min(0.0)
```

- *Fog* impacts the visibility of the vehicle, according to the analysis of its changes based on real-world weather data, we consider it realistic that the change of fog level within one hour is within 10%.

```
context Fog
inv: self.fogLevel <= (self.getPreviousValue(1h).fogLevel+0.1).max(1.0) and self
    .fogLevel >= (self.getPreviousValue(1h).fogLevel-0.1).min(0.0)
```

- *Wetness* (expressed as a percentage) reflects how the road surfaces should be. The realistic wetness level changes within an hour should be less than 5%. For example, if the current wetness level is 80%, the realistic wetness level in one hour should be between 75% and 85%.

```
context Wetness
inv: self.wetnessLevel <= (self.getPreviousValue(1h).wetnessLevel+0.05).max(1.0)
    and self.wetnessLevel >= (self.getPreviousValue(1h.wetnessLevel)-0.05).min
    (0.0)
```

- Regarding *time of day*, its changes should follow the passage of time in the real world. However, in the simulated world, the simulator has its own clock. So, we consider the passage of time to be realistic if the passage of time follows or is slower than the simulation time.

```
context TimeOfDay
def: t = secondinsimulation
inv: self.timeofday <= self.getPreviousValue(t).timeofday + t
```

³<https://openweathermap.org/>

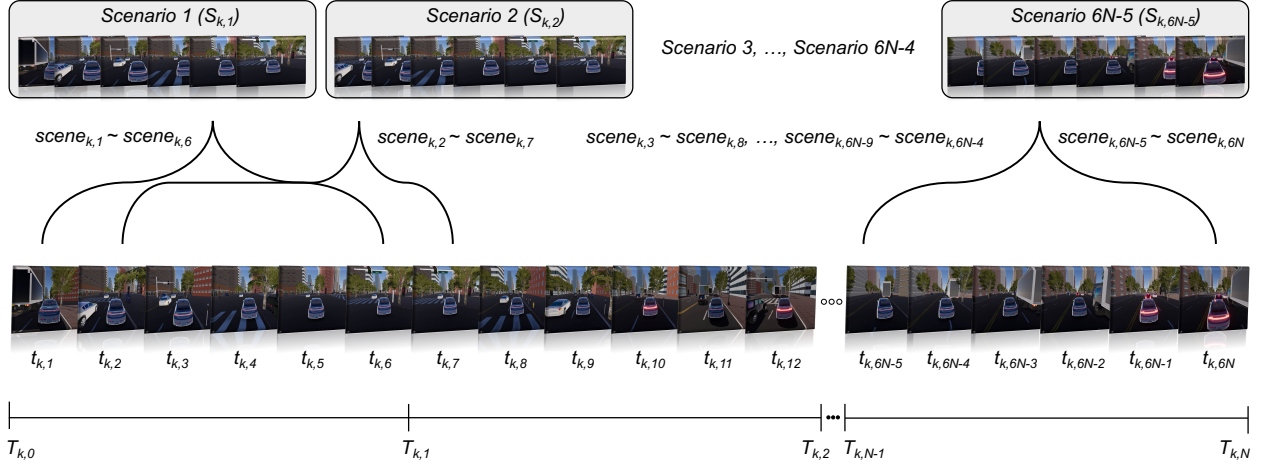


Figure 5: **The process for scenario identification in the k th execution.** k denotes the k th execution, and T is the simulation time after an environment configuration action is invoked. $scene_{k,x}$ is the x th scene captured in the k th execution.

By validating if generated scenarios satisfy the above constraints in terms of realism, we further classified the generated scenarios into four types by considering collisions, i.e., *Realistic Collision Scenarios (RCS)*, *Unrealistic Collision Scenarios (UCS)*, *Realistic Non-Collision Scenarios (RNS)*, and *Unrealistic Non-Collision Scenarios (UNS)*. For each execution k , we collected the total number of the generated test scenarios as $\#TS_k$, the number of these four types of scenarios as $\#RCS_k$, $\#UCS_k$, $\#RNS_k$, and $\#UNS_k$, and proportion of the four types out of all scenarios as $RCS\%_k$, $UCS\%_k$, $RNS\%_k$, and $UNS\%_k$. In addition, we also calculated the average time it takes for a realistic collision scenario (i.e., RCS_k) to happen as *Realistic Collision Time* (RCT_{RCS_k}).

5.4.3 Diversity Metrics

To measure *Diversity* in one execution, we defined two metrics: *API Diversity* (i.e., Div_{API}), and *Scenario Diversity* (i.e., $Div_{Scenario}$).

API Diversity (Div_{API}) measures the diversity of the environment configuration APIs invoked. Div_{API} is calculated for each execution k as $Div_{API_k} = \frac{\#UniqueAPI_k}{\#InvokedAPI_k}$, where $\#UniqueAPI_k$ represents the number of the unique environment configuration APIs invoked in execution k and $\#InvokedAPI_k$ represents the total number of the invoked APIs in execution k .

Scenario Diversity ($Div_{Scenario}$) measures the diversity of generated driving scenarios. A driving scenario (see Section 5.3.3) is regarded as a sequence of scenes over a time period, i.e.,

$$S_{k,i} = \langle scene_{k,i}^1, scene_{k,i+1}^2, \dots, scene_{k,i+n-1}^n, ST \rangle \quad (12)$$

where k is the k th execution, i is the i th scenario that occurred in the execution, $scene_{k,x}$ is the x th scene captured in the execution, n is the number of scenes in the scenario, and ST is the time period that the scenario spans. In our current design, we set ST as 3 seconds, which is the same as the simulation time (i.e., T) after invoking an environment configuration action, and capture a scene every 0.5 seconds; therefore, each scenario contains 6 scenes, i.e., $n = 6$. Figure 5 shows an example of how scenarios are identified in the k th execution. For an execution k , $Div_{Scenario}$ is calculated by comparing occurred scenarios based on the 11 properties characterizing scenes (Table 3). For each pair of scenarios (i.e., $S_{k,i}$, $S_{k,j}$ and $i \neq j$) in the k th execution, we first calculate *similarity* between $S_{k,i}$ and $S_{k,j}$ based on Algorithm 5, which is inspired by the Ratcliff-Obershelp similarity algorithm [10] which is originally designed for measuring the similarity of two strings [50]. Algorithm 5 calculates $Sim_{S_{k,i}, S_{k,j}}$ by finding a set of consecutive scenes that can maximize the similarity between $S_{k,i}$ and $S_{k,j}$:

$$Sim_{S_{k,i}, S_{k,j}} = \text{SCENARIO_SIMILARITY}(S_{k,i}, S_{k,j}), Sim_{S_{k,i}, S_{k,j}} \in [0, 1]; \quad (13)$$

then, we define their *diversity* ($Div_{S_{k,i}, S_{k,j}}$) based on the *similarity* as:

$$Div_{S_{k,i}, S_{k,j}} = 1 - Sim_{S_{k,i}, S_{k,j}}; \quad (14)$$

Scenario Diversity is calculated based on all such pairwise *diversity* of the scenarios in the k th execution as:

$$Div_{Scenario_k} = \frac{\sum_{i=1}^{m-1} \sum_{j=i+1}^m Div_{S_{k,i}, S_{k,j}}}{m}, \quad (15)$$

where m is the number of scenarios generated in execution k .

5.5 Statistical Test

To account for the randomness caused by the RL algorithm (i.e., DQN) and the ADS itself, it is essential to use statistical tests to compare the performance of different strategies [5, 38]. The selection of appropriate statistical techniques is vital to answer the RQs correctly. As suggested by Arcuri and Briand [5], we first checked if our samples are normally distributed using the Kolmogorov-Smirnov test [13], and results show that they are not normally distributed. Thus, we applied the non-parametric statistical techniques to compare samples generated by *DeepQTest* and baseline strategies.

Specifically, we use the Mann and Whitney U test [62] for assessing the statistical significance and calculate the effect size with Vargha and Delaney metric \hat{A}_{12} . Given an evaluation metric, \mathcal{M} , \hat{A}_{12} was used to compare the probability (i.e., how often) of yielding higher values of the metric \mathcal{M} for two strategies, A and B. If \hat{A}_{12} is 0.5, then they are equal. If \hat{A}_{12} is greater than 0.5, then A has a higher chance to obtain higher values of \mathcal{M} than B, and vice versa. The Mann–Whitney U test calculates a p -value to determine if the performance difference between A and B is significant. A p -value less than 0.05 indicates the significant difference between A and B. In addition, by following the guidelines proposed by Kitchenham et al. [48], we divide the Vargha and Delaney effect size magnitude of \hat{A}_{12} into four levels: *negligible* ($\hat{A}_{12} \in (0.444, 0.556)$), *small* ($\hat{A}_{12} \in [0.556, 0.638)$ or $(0.362, 0.444]$), *medium* ($\hat{A}_{12} \in [0.638, 0.714)$ or $(0.286, 0.362]$), *large* ($\hat{A}_{12} \in [0.714, 1.0]$ or $[0, 0.286]$).

In addition to investigating the performance of different strategies, we also want to investigate the correlation among the three selected measures, i.e., *TTC*, *DTO*, *Jerk*. We choose to use Spearman’s rank correlation (ρ) test, which is a non-parametric, rank-based assessment of correlation test. The ρ value ranges from -1.0 to 1.0 , i.e., there is a positive correlation if ρ is close to 1.0 and a negative correlation when ρ closes to -1.0 . If ρ is closer to 0 , then there is no correlation between the two measures. We also reported the significance of the correlation using a p -value, i.e., a p -value less than 0.05 tells that the correlation is statistically significant.

6 Experiment Results and Analysis

6.1 Results for RQ1

To answer RQ1, we compare each of the three reward settings of *DeepQTest* (i.e., *DeepQTest_{TTC}*, *DeepQTest_{DTO}*, *DeepQTest_{Jerk}*) with the *RS* and *GS* strategies. We repeated the experiment 20 times under all real-world weather conditions on all roads (i.e., 20 runs \times 4 real-world weather conditions \times 4 roads = 320 samples for each of the three strategies). The comparison analysis was performed with *Safety and Comfort Metrics* using the Mann and Whitney U test and Vargha and Delaney effect size. Results are summarized in Table 4, and the detailed statistical results on each road for the three reward settings can be seen in Table 10, 11, and 12 in Appendix 8.

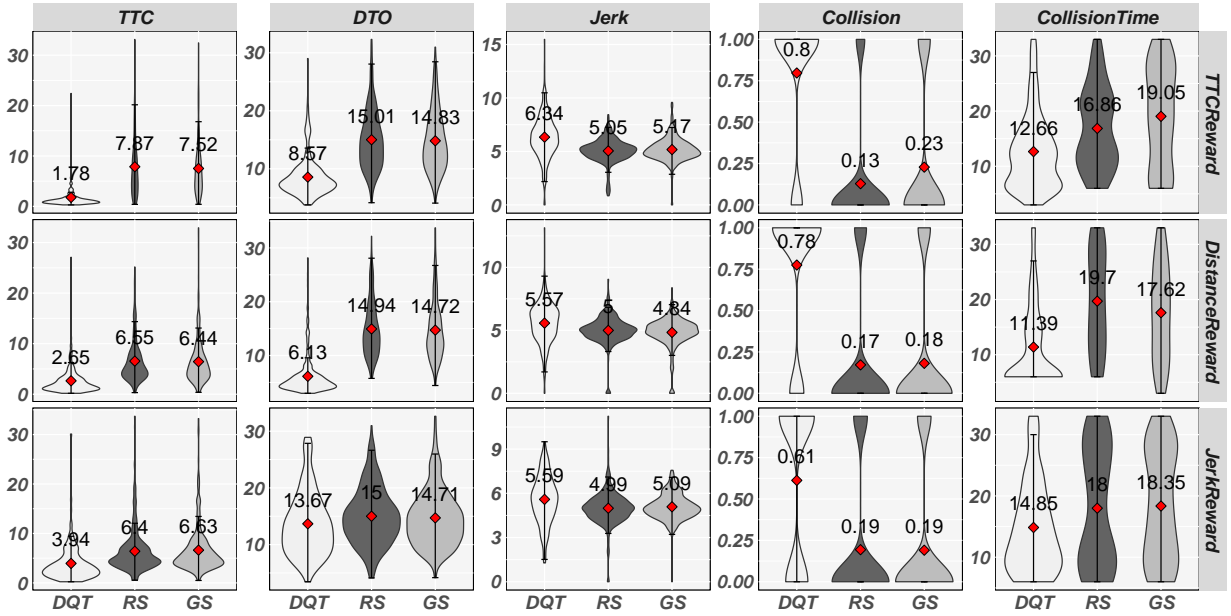
As can be seen from Table 4, *DeepQTest* with all settings significantly outperformed *RS* and *GS* in terms of all metrics. In terms of \hat{A}_{12} , we found that for *TTC*, and *CollisionTime*, \hat{A}_{12} is at *large* magnitude level (i.e., ≥ 0.714 or ≤ 0.286) for all the cases. For *DTO*, \hat{A}_{12} is at the *large* magnitude level (i.e., ≤ 0.286) except for *DeepQTest_{Jerk}* with which we observed the *small* magnitude level results. For *Jerk*, \hat{A}_{12} is at least at the *large* magnitude level (i.e., ≥ 0.714) for *DeepQTest_{TTC}*, the *medium* magnitude level (i.e., ≥ 0.638) for *DeepQTest_{DTO}*, and the *small* magnitude level for *DeepQTest_{Jerk}* (i.e., ≥ 0.556). For the *#Collision* metric, we can observe that \hat{A}_{12} is at the *large* magnitude level (i.e., ≥ 0.714) for *DeepQTest_{TTC}* and *DeepQTest_{DTO}*, and at *medium* magnitude level (i.e., ≥ 0.638) for *DeepQTest_{Jerk}*.

In addition, to study the distributions of each metric, we present violin plots for *DeepQTest*, *RS*, and *GS* for each reward setting in Figure 6. From the figure, we can observe that all settings of *DeepQTest* outperformed *RS* and *GS* in terms of the average values (red dots in Figure 6) of all evaluation metrics. We looking at the distributions, we can see that *DeepQTest* achieved less variability, except for *Jerk*, implying that *DeepQTest* performed more stably in terms of *TTC*, *DTO*, *#Collision*, and *CollisionTime*. For *Jerk*, although *DeepQTest* performed less stably, it still achieved higher *Jerk* values on average. One plausible explanation is that *DeepQTest_{Jerk}* may not be as effective as *DeepQTest_{TTC}*, *DeepQTest_{DTO}* in terms of training a stable *DeepQTest* model. More discussions about this observation will be provided in Section 6.2.

Table 4: Results of pair comparison of *DeepQTest* and RS/GS in terms of *Safety and Comfort Metrics* using the Vargha and Delaney statistics and the Mann–Whitney U test - RQ1

<i>DeepQTest</i> vs. (RS, GS)		TTC		DTO		Jerk		#Collision		CollisionTime	
		\hat{A}_{12}	p	\hat{A}_{12}	p	\hat{A}_{12}	p	\hat{A}_{12}	p	\hat{A}_{12}	p
<i>DeepQTest</i> _{TTC}	GS	0.095	<0.05	0.117	<0.05	0.735	<0.05	0.834	<0.05	0.149	<0.05
	RS	0.091	<0.05	0.125	<0.05	0.724	<0.05	0.784	<0.05	0.179	<0.05
<i>DeepQTest</i> _{DTO}	GS	0.172	<0.05	0.058	<0.05	0.639	<0.05	0.802	<0.05	0.162	<0.05
	RS	0.186	<0.05	0.064	<0.05	0.661	<0.05	0.797	<0.05	0.176	<0.05
<i>DeepQTest</i> _{Jerk}	GS	0.285	<0.05	0.422	<0.05	0.635	<0.05	0.709	<0.05	0.279	<0.05
	RS	0.269	<0.05	0.437	<0.05	0.619	<0.05	0.711	<0.05	0.274	<0.05

* p is p -value; a bold \hat{A}_{12} with a $p < 0.05$ implies that *DeepQTest* is significantly better than GS/RS. \hat{A}_{12} magnitude: *negligible* ($\hat{A}_{12} \in (0.444, 0.556)$), *small* ($\hat{A}_{12} \in [0.556, 0.638)$ or $(0.362, 0.444]$), *medium* ($\hat{A}_{12} \in [0.638, 0.714)$ or $(0.286, 0.362]$), *large* ($\hat{A}_{12} \in [0.714, 1.0]$ or $[0, 0.286]$).



* DQT: *DeepQTest*; RS: *Random Strategy*; GS: *Greedy Strategy*.

Figure 6: Descriptive statistics of the evaluation metrics achieved by *DeepQTest*, RS and GS– RQ1

Conclusion for RQ1: Compared to RS and GS, *DeepQTest* achieved significant improvements in terms of all *Safety and Comfort Metrics*. This represents that *DeepQTest* is more effective in generating environment configurations that lead to shorter time to collide with obstacles (*TTC*), shorter distance to obstacles (*DTO*), a lower degree of passenger comfort (*Jerk*), and more collision occurrences (*#Collision*), and shorter (*CollisionTime*). In summary, the problem we address is complex enough, which cannot effectively be addressed with RS and GS.

6.2 Results for RQ2

To answer RQ2, we compare the performance achieved by each of the models under three reward function settings (i.e., *DeepQTest*_{TTC}, *DeepQTest*_{DTO}, *DeepQTest*_{Jerk}) on all four roads for each weather condition (i.e., *RD*, *RN*, *SD*, *SN*). We repeated the experiment 20 times. Thus, for each weather condition, there are in total of 80 (i.e., 20 runs \times 4 Roads) samples for each reward function. Table 5 reports the results of pair-wise comparisons of the three reward functions in terms of *Safety and Comfort Metrics* and *Diversity Metrics* for each weather condition. More detailed results for each road can be found in Table 13 in Appendix.

Regarding *Safety and Comfort Metrics*, for all the weather conditions, we found that *DeepQTest*_{TTC} and *DeepQTest*_{DTO} consistently achieved the best performance; *DeepQTest*_{TTC} is the most effective in generating

Table 5: Results of pair comparisons among the three reward functions in terms of *Safety and Comfort Metrics and Diversity Metrics* using the Vargha and Delaney statistics and the Mann–Whitney U test - RQ2

Reward Comparison		TTC		DTO		Jerk		#Collision		CollisionTime		Div _{API}		Div _{Scenario}	
		\hat{A}_{12}	p	\hat{A}_{12}	p	\hat{A}_{12}	p	\hat{A}_{12}	p	\hat{A}_{12}	p	\hat{A}_{12}	p	\hat{A}_{12}	p
DeepQTest _{TTC} _{RD}	DeepQTest _{DTO} _{RD}	0.281	<0.05	0.789×	<0.05	0.606	<0.05	0.525	0.475	0.499	0.980	0.530	0.503	0.461	0.475
	DeepQTest _{Jerk} _{RD}	0.210	<0.05	0.228	<0.05	0.621	<0.05	0.562	0.086	0.409	<0.05	0.420	0.079	0.374×	<0.05
DeepQTest _{DTO} _{RD}	DeepQTest _{Jerk} _{RD}	0.332	<0.05	0.117	<0.05	0.529	0.533	0.537	0.314	0.411	<0.05	0.388×	<0.05	0.412×	<0.05
	DeepQTest _{DTO} _{RD}	0.297	<0.05	0.811×	<0.05	0.625	<0.05	0.475	0.442	0.571	0.111	0.610	<0.05	0.568	0.094
DeepQTest _{TTC} _{RN}	DeepQTest _{DTO} _{RN}	0.247	<0.05	0.177	<0.05	0.609	<0.05	0.600	<0.05	0.366	<0.05	0.409×	<0.05	0.378×	<0.05
	DeepQTest _{Jerk} _{RN}	0.432	<0.05	0.067	<0.05	0.501	0.984	0.625	<0.05	0.309	<0.05	0.306×	<0.05	0.317×	<0.05
DeepQTest _{DTO} _{RN}	DeepQTest _{DTO} _{RN}	0.297	<0.05	0.811×	<0.05	0.625	<0.05	0.475	0.442	0.571	0.111	0.610	<0.05	0.568	0.094
	DeepQTest _{Jerk} _{RN}	0.247	<0.05	0.177	<0.05	0.609	<0.05	0.600	<0.05	0.366	<0.05	0.409×	<0.05	0.378×	<0.05
DeepQTest _{TTC} _{SD}	DeepQTest _{DTO} _{SD}	0.304	<0.05	0.826×	<0.05	0.636	<0.05	0.525	0.421	0.535	0.435	0.553	0.235	0.527	0.639
	DeepQTest _{Jerk} _{SD}	0.185	<0.05	0.188	<0.05	0.650	<0.05	0.606	<0.05	0.344	<0.05	0.365×	<0.05	0.386×	<0.05
DeepQTest _{DTO} _{SD}	DeepQTest _{Jerk} _{SD}	0.346	<0.05	0.073	<0.05	0.524	0.604	0.581	<0.05	0.325	<0.05	0.330×	<0.05	0.360×	<0.05
	DeepQTest _{DTO} _{SD}	0.304	<0.05	0.826×	<0.05	0.636	<0.05	0.525	0.421	0.535	0.435	0.553	0.235	0.527	0.639
DeepQTest _{TTC} _{SN}	DeepQTest _{DTO} _{SN}	0.371	<0.05	0.787×	<0.05	0.625	<0.05	0.519	0.551	0.536	0.417	0.529	0.523	0.490	0.832
	DeepQTest _{Jerk} _{SN}	0.185	<0.05	0.182	<0.05	0.581	0.078	0.600	<0.05	0.339	<0.05	0.323×	<0.05	0.338×	<0.05
DeepQTest _{DTO} _{SN}	DeepQTest _{Jerk} _{SN}	0.347	<0.05	0.082	<0.05	0.457	0.352	0.581	<0.05	0.335	<0.05	0.333×	<0.05	0.349×	<0.05
	DeepQTest _{DTO} _{SN}	0.347	<0.05	0.082	<0.05	0.457	0.352	0.581	<0.05	0.335	<0.05	0.333×	<0.05	0.349×	<0.05

* RD: Rainy Day; RN: Rainy Night; SD: Sunny Day; SN: Sunny Night; p is p -value; a bold \hat{A}_{12} with a $p < 0.05$ implies that the former model is significantly better than the latter, whereas a \hat{A}_{12} decorated by symbol "x" indicates the former model performed significantly worse than the latter; a $p > 0.5$ means no significant difference between two models. \hat{A}_{12} magnitude: *negligible* ($\hat{A}_{12} \in (0.444, 0.556)$), *small* ($\hat{A}_{12} \in [0.556, 0.638)$ or $(0.362, 0.444)$), *medium* ($\hat{A}_{12} \in [0.638, 0.714)$ or $(0.286, 0.362]$), *large* ($\hat{A}_{12} \in [0.714, 1.0]$ or $[0, 0.286]$).

environment configurations that lead to less time for AVUT to collide with obstacles (*TTC*) while *DeepQTest_{DTO}* is the most effective in generating environment configurations that lead to less distance between AVUT and obstacles (*DTO*), as expected. For *Jerk*, it is surprising that the best results are achieved by *DeepQTest_{TTC}* but not *DeepQTest_{Jerk}*. Recall that *Jerk* is calculated as the rate of changes of acceleration, therefore, to figure out the reason that *DeepQTest_{TTC}* outperformed *DeepQTest_{Jerk}*, we further analyzed the changes in acceleration and the corresponding *Jerk* values by checking scenarios generated by *DeepQTest_{Jerk}* and *DeepQTest_{TTC}*. We found that *DeepQTest_{Jerk}* generates scenarios that result in higher *Jerk* over a period of time. For instance, a sequence of *acceleration (m/s²)/Jerk* values over a period of time can be:

$$T_0: 2.70/2.44, T_1: 0.70/3.82, T_2: -2.22/6.12, T_3: 1.73/10.42.$$

However, *DeepQTest_{TTC}* could generate scenarios where AVUT collides with obstacles in a less period of time, and such scenarios would likely result in a higher *Jerk* value, i.e., a lower degree of comfort for passengers. For instance, in a run of *DeepQTest_{TTC}*, a sequence of *acceleration (m/s²)/Jerk* values over three steps is:

$$T_0: 3.30/4.64, T_1: -0.91/8.58, T_2: 2.18/8.02.$$

There might exist correlations among reward functions based on their corresponding metrics. To study the correlations, for each reward function, we calculated *TTC*, *DTO*, *Jerk* at each step for all 20 runs on all of the four roads, then analyzed results using Spearman's rank correlation (ρ) test. Results show a significantly positive correlation between *TTC* and *DTO* (i.e., $p < 0.05$ and $\rho = 0.423$), and significantly negative correlations observed in *TTC-Jerk* (i.e., $p < 0.05$ and $\rho = -0.254$) and *DTO-Jerk* (i.e., $p < 0.05$ and $\rho = -0.292$). It indicates that a lower *TTC* (less time to collide with obstacles) would lead to a lower *DTO* (i.e., less distance to obstacles) and a higher *Jerk* (i.e., a lower degree of comfort).

In addition, we observed similar pair comparison results among reward functions for metrics *#Collision* and *CollisionTime*. No significant difference is observed between *DeepQTest_{TTC}* and *DeepQTest_{DTO}* under all four kinds of weather conditions. Both *DeepQTest_{TTC}* and *DeepQTest_{DTO}* outperformed *DeepQTest_{Jerk}* consistently on the four weather conditions, and the differences are significant on *RN*, *SD*, and *SN*. It indicates that reward functions based on *TTC* and *DTO* might have more chances to guide RL to introduce environment configurations that result in collisions.

In Table 5, we also analyzed the diversity among the scenarios generated by each reward function in each weather condition. Results show that *DeepQTest_{Jerk}* performed the best in terms of both diversity-related metrics, i.e., invoking more diverse APIs (*Div_{API}*) and generating more diverse scenarios (*Div_{Scenario}*). More specifically, *DeepQTest_{Jerk}* outperformed *DeepQTest_{TTC}* and *DeepQTest_{DTO}* in terms of *Div_{API}* and *Div_{Scenario}* in all weather conditions, except *Div_{API}* in *RD*. As for *Div_{API}* in *RD*, *DeepQTest_{Jerk}* outperformed *DeepQTest_{DTO}*, and *DeepQTest_{Jerk}* and *DeepQTest_{TTC}* performed equivalently in statistics. Regarding *DeepQTest_{TTC}* and *DeepQTest_{DTO}*, there is no significant difference in terms of *Div_{API}* and *Div_{Scenario}*. But in terms of *Div_{API}*, *DeepQTest_{TTC}* is slightly better than *DeepQTest_{DTO}* as \hat{A}_{12} of comparing *DeepQTest_{TTC}* with *DeepQTest_{DTO}* is greater 0.5 in all weather conditions.

Table 6: Ranking of $DeepQTest_{TTC}$, $DeepQTest_{DTO}$, and $DeepQTest_{Jerk}$ in terms of metrics and real-world weather conditions - RQ2

	<i>TTC</i>	<i>DTO</i>	<i>Jerk</i>	<i>#Collision</i>	<i>CollisionTime</i>	<i>DIV_{API}</i>	<i>DIV_{Scenario}</i>
<i>RD</i>	DQT_T, DQT_D, DQT_J	DQT_D, DQT_T, DQT_J	$DQT_T, DQT_D/DQT_J$	$DQT_T/DQT_D/DQT_J$	$DQT_D/DQT_T, DQT_J$	$DQT_J, DQT_T/DQT_D$	$DQT_J, DQT_D/DQT_T$
<i>RN</i>	DQT_T, DQT_D, DQT_J	DQT_D, DQT_T, DQT_J	$DQT_T, DQT_J/DQT_D$	$DQT_D/DQT_T, DQT_J$	$DQT_T/DQT_D, DQT_J$	$DQT_J, DQT_T/DQT_D$	$DQT_J, DQT_T/DQT_D$
<i>SD</i>	DQT_T, DQT_D, DQT_J	DQT_D, DQT_T, DQT_J	$DQT_T, DQT_D/DQT_J$	$DQT_T/DQT_D, DQT_J$	$DQT_T/DQT_D, DQT_J$	$DQT_J, DQT_T/DQT_D$	$DQT_J, DQT_T/DQT_D$
<i>SN</i>	DQT_T, DQT_D, DQT_J	DQT_D, DQT_T, DQT_J	$DQT_T, DQT_J/DQT_D$	$DQT_T/DQT_D, DQT_J$	$DQT_T/DQT_D, DQT_J$	$DQT_J, DQT_T/DQT_D$	$DQT_J, DQT_D/DQT_T$
<i>Rec_M</i>	DQT_T	DQT_D	DQT_T	DQT_T	DQT_T	DQT_J	DQT_J

* DQT_T : $DeepQTest_{TTC}$, DQT_D : $DeepQTest_{DTO}$, DQT_J : $DeepQTest_{Jerk}$. *RD*: Rainy Day; *RN*: Rainy Night; *SD*: Sunny Day; *SN*: Sunny Night; a reward function before "," is statistically significantly better than the reward function after ","; a "/" means two reward functions have no statistically significant difference, and a reward function before "/" achieved better (or the same) performance than the reward function after "/" in terms of mean metric values. *Rec_M*: recommended by metric.

Based on Table 5, we summarized the results obtained by the three reward functions in each weather condition for each metric using ranking and provided a recommendation of reward function for each metric in Table 6. For all metrics, we found that the ranking results of the three reward functions do not vary much in weather conditions. $DeepQTest_{TTC}$ achieved the overall best performance in terms of all metrics.

Conclusion for RQ2: Among all three reward functions (i.e., $DeepQTest_{TTC}$, $DeepQTest_{DTO}$, and $DeepQTest_{Jerk}$), $DeepQTest_{TTC}$ achieved the overall best performance. Regarding *Safety and Comfort Metrics*, $DeepQTest_{TTC}$ performed the best in terms of *TTC* and *Jerk*, and the second best in terms of *DTO*. As for *#Collision* and *CollisionTime*, $DeepQTest_{TTC}$ and $DeepQTest_{DTO}$ both performed the best. Regarding *Diversity Metrics*, $DeepQTest_{Jerk}$ performed the best, followed by $DeepQTest_{TTC}$.

6.3 Results for RQ3

To answer RQ3, we compared $DeepQTest$ with $DeepCollision$ [58] regarding *Realism Metrics* and *Diversity Metrics*. Table 7 reports results of scenarios in terms of realism along with the occurrence of collisions, achieved by the best reward function (i.e., $DeepQTest_{TTC}$) and $DeepCollision$ on all of the four roads (i.e., *R1*–*R4*) under the four weather conditions (i.e., $DeepQTest_{TTC_{RD}}$, $DeepQTest_{TTC_{RN}}$, $DeepQTest_{TTC_{SD}}$, $DeepQTest_{TTC_{SN}}$). Table 8 represents the results of pair comparisons of $DeepQTest_{TTC}$ and $DeepCollision$ using Vargha and Delaney statistics (\hat{A}_{12}) and the Mann–Whitney U test (*p*-value).

The termination criterion of $DeepCollision$ is either to reach the specified destination or to run out of the specified time budget, which allows AVUT to continue driving even if a collision happens. But, for $DeepQTest$, besides reaching the destination or running out of the budget, it also terminates testing once a collision occurs. Thus, compared to $DeepQTest$, $DeepCollision$ generates more test scenarios, as shown in column *#TS* in Table 7.

As for *Realism Metrics*, based on results shown in Table 7, all scenarios generated by $DeepQTest_{TTC}$ are realistic scenarios (with *RCS %* and *RNS %* being 100%, and unrealistic scenarios with *UCS %* and *UNS %* being 0%). This is because $DeepQTest$ is designed by considering realistic constraints (Section 4.2), and all scenarios generated by $DeepQTest$ conform to these constraints. Instead, $DeepCollision$ achieved a limited performance in generating realistic scenarios on *R1*, *R3*, and *R4*: the percentages of generated realistic scenarios (*RCS %* and *RNS %*) are 40.93% (0.55% + 40.38%), 3.49% (0.38% + 3.44%) and 2.68% (0.04% + 2.64%), respectively. On *R2*, $DeepCollision$ generated 89.36% realistic scenarios out of the 3440 scenarios.

Regarding realistic collision scenarios, $DeepQTest_{TTC}$ generated more realistic collision scenarios (*#RCS*) than $DeepCollision$ on *R2*, *R3* and *R4*. Especially for *R3* and *R4*, with 20 runs, $DeepQTest_{TTC}$ generated a minimum of 13 and a maximum of 18 realistic collision scenarios, while $DeepCollision$ produced only 2 realistic collision scenarios. On *R1*, although $DeepCollision$ generated 19 realistic collision scenarios, the percentage of realistic collision scenarios (i.e., *RCS %* = 0.55%) is much smaller than that for $DeepQTest$ (i.e., at least 2.02%), implying that on *R1*, $DeepCollision$ needed to generate a higher number of scenarios (3440) to get a comparable number of realistic collision scenarios as $DeepQTest$. Besides, the proportions of collision scenarios among all realistic scenarios achieved by $DeepCollision$ are all lower than $DeepQTest$. In addition, the significant outperformance of $DeepQTest$ over $DeepCollision$, with large effect size magnitude, can be observed in Table 8, indicated as *p*-value < 0.05 and $\hat{A}_{12} > 0.825$. On *R1*, $DeepCollision$ generated the most realistic collision scenarios (i.e., 19), but the difference is modest (i.e., 19 vs. 16) and not significant (i.e., *p*-value > 0.05 and $\hat{A}_{12} \in [0.425, 0.450]$). Note that the low percentage of realistic collision scenarios (*RCS %*) by $DeepQTest_{TTC}$ (i.e., the maximum is 3.44% with $DeepQTest_{TTC_{SD}}$ on *R3*) relates to how we identify and collect test scenarios. As a change in the operating environment can impact ADS continuously in the real world, we identify a test scenario with a time span *ST* that is composed of a successive sequence of *scenes* (see Equation 12),

Table 7: Results of a number of test scenarios ($\#TS$), a number/percentage of realistic collision scenarios ($\#RCS/\%$), average time spent on observing each realistic collision scenario (CT_{RCS} seconds), a number/percentage of unrealistic collision scenarios ($\#UNS/\%$), a number/percentage of realistic non-collision scenarios ($\#RNS/\%$) and a number/percentage of unrealistic non-collision scenarios ($\#RCS/\%$) achieved by *DeepQTest_{TTC}* and *DeepCollision*.

DeepQTest vs. DeepCollision	Collision						Non-Collision					
	#TS	#RCS/%	CT_{RCS}	#UCS/%	#RNS/%	#UNS/%	#TS	#RCS/%	CT_{RCS}	#UCS/%	#RNS/%	#UNS/%
	R1						R2					
<i>DeepQTest_{TTC}_{RD}</i>	770	16/2.08%	12.40	0/0%	754/97.92%	0/0%	614	15/2.44%	15.67	0/0%	599/97.56%	0/0%
<i>DeepQTest_{TTC}_{RN}</i>	794	16/2.02%	12.00	0/0%	778/97.98%	0/0%	548	17/3.10%	8.20	0/0%	531/96.90%	0/0%
<i>DeepQTest_{TTC}_{SD}</i>	662	16/2.42%	9.92	0/0%	646/97.58%	0/0%	602	16/2.66%	11.14	0/0%	586/97.34%	0/0%
<i>DeepQTest_{TTC}_{SN}</i>	680	17/2.50%	12.00	0/0%	663/97.50%	0/0%	548	17/3.10%	11.44	0/0%	531/96.90%	0/0%
<i>DeepCollision</i>	3440	19/0.55%	18.00	23/0.67%	1389/40.38%	2009/58.40%	3440	13/0.38%	18.00	9/0.26%	3061/88.98%	357/10.38%
	R3						R4					
<i>DeepQTest_{TTC}_{RD}</i>	770	14/1.82%	8.67	0/0%	756/98.18%	0/0%	662	17/2.57%	9.60	0/0%	645/97.43%	0/0%
<i>DeepQTest_{TTC}_{RN}</i>	764	13/1.70%	10.71	0/0%	751/98.30%	0/0%	752	15/1.99%	9.92	0/0%	737/98.01%	0/0%
<i>DeepQTest_{TTC}_{SD}</i>	524	18/3.44%	7.50	0/0%	506/96.56%	0/0%	536	17/3.17%	9.00	0/0%	519/96.83%	0/0%
<i>DeepQTest_{TTC}_{SN}</i>	644	16/2.48%	7.33	0/0%	628/97.52%	0/0%	680	16/2.35%	13.67	0/0%	664/97.65%	0/0%
<i>DeepCollision</i>	4220	2/0.05%	21.00	94/2.23%	145/3.44%	3979/94.29%	4700	2/0.04%	30.00	145/3.09%	124/2.64%	4429/94.23%

* R1: Road1; R2: Road2; R3: Road3; R4: Road4. RD: Rainy Day; RN: Rainy Night; SD: Sunny Day; SN: Sunny Night. #TS: Total Scenarios; RCS: Realistic Collision Scenario; CT_{RCS} : realistic collision time for RCS; UCS: Unrealistic Collision Scenario; RNS: Realistic Non-Collision Scenario, UNS: Unrealistic Non-Collision Scenario.

then collect test scenarios every time step (t) in one execution (see an example in Figure 5). Such identification and collection aim to depict the test scenarios over time in detail, but it increases the number of collected test scenarios. Thus, it might result in low RCS % as one execution by *DeepQTest* can observe at maximum one collision scenario.

We further analyzed the average realistic collision time (i.e., CT_{RCS}). Based on CT_{RCS} in Tables 7 and 8, *DeepQTest_{TTC}* significantly outperformed *DeepCollision* on all four roads, i.e., *DeepQTest_{TTC}* took less time to generate realistic scenarios that can lead to collisions than *DeepCollision*. For example, one can observe from Table 7 that on R1, *DeepCollision* took on average 18 seconds to find a realistic collision scenario, while *DeepQTest* took on average 11.58 seconds (maximum 12.4 with *DeepQTest_{TTC}_{RD}*, and minimum 9.92 with *DeepQTest_{TTC}_{SD}*).

Regarding the effectiveness of *DeepQTest* in terms of triggering realistic collision scenarios, we found that, with the results on four roads under four weather conditions, *DeepQTest_{TTC}* identified on average 16 realistic collision scenarios out of 20 runs (i.e., $16/20=80\%$ per run), and it took on average 10.58 seconds per realistic collision scenario.

Moreover, we studied unrealistic scenarios generated by *DeepCollision* by replaying them on the four roads. We found that the generation of unrealistic scenarios is mainly caused by the four types of unrealistic environment configurations, i.e., *Unrealistic Time Changes (UTC)*, *Unrealistic Weather Changes (UWC)*, *Violation of Safety Distance (VSD)*, and *Overlapping Areas (OA)*. Examples of each type are shown in Figure 7. We further explain the four types of unrealistic environment configurations as follows:

- *Unrealistic Time Changes (UTC)* refers to the unrealistic manipulation of time changes. As Figure 7a shows, the time was manipulated and suddenly changed from the day (12 am) to the night (8 pm), which caused the AVUT to collide with the pedestrian in front.
- *Unrealistic Weather Changes (UWC)* refers to unrealistic weather changes. As shown in Figure 7b, an environment configuration action could immediately shift the weather condition from sunny to foggy. As the foggy weather condition affects the visibility of AVUT, such an instant change might leave less time for AVUT to react and hence lead to collisions (e.g., colliding with the vehicle in the front in Figure 7b). Considering that the weather condition changes over a period of time, such a sudden change is unrealistic.
- *Violation of Safety Distance (VSD)* happens when obstacles (e.g., NPC vehicles, pedestrians) are generated with initial positions violating the safety distances of AVUT from the obstacles. For testing purposes, we could introduce new obstacles into the driving environment. But such an introduction should be in accord with real-world scenarios. For instance, it is impossible for a truck to suddenly appear beside AVUT (Figure 7c). In such a case, AVUT did not have time to react and therefore collided with the truck. As driving tasks on R3 and R4 need to go through a T-junction and then turn left from a four-lane road to another four-lane road at the beginning (see Figure 4), we found that *DeepCollision* generated many collision scenarios by introducing new obstacles when AVUT was turning left or entering the new lane. This is a reason why most of the collision scenarios on R3 and R4 are unrealistic (see Table 7).
- *Overlapping Areas (OA)* is the case that an obstacle is generated in an area overlapping the areas covered by the AVUT and the newly introduced obstacles due to a lack of consideration of the volume of the new obstacles. Such introductions will directly lead to collisions. Figure 7d is an example of a collision caused by

Table 8: Results of pair comparisons of $DeepQTest_{TTC}$ and $DeepCollision$ using Vargha and Delaney statistics (\hat{A}_{12}) and the Mann–Whitney U test (p -value) in terms of a number/percentage of realistic collision scenarios ($\#RCS/\%$), average realistic collision time (CT_{RCS} seconds), a number/percentage of unrealistic collision scenarios ($\#UNS/\%$), a number/percentage of realistic non-collision scenarios ($\#RNS/\%$) and a number/percentage of unrealistic non-collision scenarios ($\#RCS/\%$).

$DeepQTest_{TTC}$ vs. $DeepCollision$	Collision								Non-Collision									
	#RCS		RCS %		CT_{RCS}		#UCS		UCS %		#RNS		RNS %		#UNS		RNS %	
	\hat{A}_{12}	p	\hat{A}_{12}	p	\hat{A}_{12}	p	\hat{A}_{12}	p	\hat{A}_{12}	p	\hat{A}_{12}	p	\hat{A}_{12}	p	\hat{A}_{12}	p	\hat{A}_{12}	p
R1																		
$DeepQTest_{TTC_{RD}}$	0.425	0.164	0.805	<0.05	0.174	<0.05	0.150	<0.05	0.150	<0.05	0.255x	<0.05	1.000	<0.05	0.000	<0.05	0.000	<0.05
$DeepQTest_{TTC_{RN}}$	0.425	0.164	0.805	<0.05	0.188	<0.05	0.150	<0.05	0.150	<0.05	0.285x	<0.05	1.000	<0.05	0.000	<0.05	0.000	<0.05
$DeepQTest_{TTC_{SD}}$	0.425	0.164	0.805	<0.05	0.201	<0.05	0.150	<0.05	0.150	<0.05	0.172x	<0.05	1.000	<0.05	0.000	<0.05	0.000	<0.05
$DeepQTest_{TTC_{SN}}$	0.450	0.310	0.854	<0.05	0.130	<0.05	0.150	<0.05	0.150	<0.05	0.203x	<0.05	1.000	<0.05	0.000	<0.05	0.000	<0.05
R2																		
$DeepQTest_{TTC_{RD}}$	0.550	0.506	0.794	<0.05	0.340	<0.05	0.300	<0.05	0.300	<0.05	0.016x	<0.05	0.635	0.141	0.075	<0.05	0.075	<0.05
$DeepQTest_{TTC_{RN}}$	0.600	0.154	0.876	<0.05	0.151	<0.05	0.300	<0.05	0.300	<0.05	0.018x	<0.05	0.629	0.164	0.075	<0.05	0.075	<0.05
$DeepQTest_{TTC_{SD}}$	0.575	0.302	0.835	<0.05	0.194	<0.05	0.300	<0.05	0.300	<0.05	0.015x	<0.05	0.701	<0.05	0.075	<0.05	0.075	<0.05
$DeepQTest_{TTC_{SN}}$	0.600	0.154	0.876	<0.05	0.138	<0.05	0.300	<0.05	0.300	<0.05	0.010x	<0.05	0.751	<0.05	0.075	<0.05	0.075	<0.05
R3																		
$DeepQTest_{TTC_{RD}}$	0.850	<0.05	0.850	<0.05	0.275	<0.05	0.000	<0.05	0.000	<0.05	0.800	<0.05	1.000	<0.05	0.000	<0.05	0.000	<0.05
$DeepQTest_{TTC_{RN}}$	0.825	<0.05	0.825	<0.05	0.325	<0.05	0.000	<0.05	0.000	<0.05	0.723	<0.05	1.000	<0.05	0.000	<0.05	0.000	<0.05
$DeepQTest_{TTC_{SD}}$	0.950	<0.05	0.950	<0.05	0.350	<0.05	0.000	<0.05	0.000	<0.05	0.738	<0.05	1.000	<0.05	0.000	<0.05	0.000	<0.05
$DeepQTest_{TTC_{SN}}$	0.900	<0.05	0.900	<0.05	0.275	<0.05	0.000	<0.05	0.000	<0.05	0.723	<0.05	1.000	<0.05	0.000	<0.05	0.000	<0.05
R4																		
$DeepQTest_{TTC_{RD}}$	0.925	<0.05	0.925	<0.05	0.375	<0.05	0.000	<0.05	0.000	<0.05	0.850	<0.05	1.000	<0.05	0.000	<0.05	0.000	<0.05
$DeepQTest_{TTC_{RN}}$	0.875	<0.05	0.875	<0.05	0.175	<0.05	0.000	<0.05	0.000	<0.05	0.900	<0.05	1.000	<0.05	0.000	<0.05	0.000	<0.05
$DeepQTest_{TTC_{SD}}$	0.925	<0.05	0.925	<0.05	0.375	<0.05	0.000	<0.05	0.000	<0.05	0.805	<0.05	1.000	<0.05	0.000	<0.05	0.000	<0.05
$DeepQTest_{TTC_{SN}}$	0.900	<0.05	0.900	<0.05	0.275	<0.05	0.000	<0.05	0.000	<0.05	0.835	<0.05	1.000	<0.05	0.000	<0.05	0.000	<0.05

* R1: Road1; R2: Road2; R3: Road3; R4: Road4. RD: Rainy Day; RN: Rainy Night; SD: Sunny Day; SN: Sunny Night. RCS: Realistic Collision Scenario; UCS: Unrealistic Collision Scenario; RNS: Realistic Non-Collision Scenario, UNS: Unrealistic Non-Collision Scenario. p is p -value; a bold \hat{A}_{12} with a $p < 0.05$ implies that $DeepQTest^*$ is significantly better than $DeepCollision$, whereas a \hat{A}_{12} decorated by symbol "x" indicates $DeepQTest^*$ performed significantly worse than $DeepCollision$; a $p > 0.5$ means no significant difference between $DeepQTest^*$ and $DeepCollision$. \hat{A}_{12} magnitude: negligible ($\hat{A}_{12} \in (0.444, 0.556)$), small ($\hat{A}_{12} \in [0.556, 0.638)$ or $(0.362, 0.444]$), medium ($\hat{A}_{12} \in [0.638, 0.714)$ or $(0.286, 0.362]$), large ($\hat{A}_{12} \in [0.714, 1.0]$ or $[0, 0.286]$).

generating a truck in the same area of AVUT. Such introductions of obstacles might mislead the approach by introducing large obstacles such as trucks.

Furthermore, we compared $DeepQTest_{TTC}$ and $DeepCollision$ in terms of *Diversity Metrics*. $DeepQTest$ achieved an overall better performance than $DeepCollision$ in terms of *Diversity Metrics*. Results of the pair-wise comparison are shown in Table 9. In terms of Div_{API} , we found that $DeepQTest_{TTC}$ achieved significantly better results than $DeepCollision$, which indicates that, compared to $DeepCollision$, $DeepQTest_{TTC}$ could test AVUT under more diverse combinations of environment configurations in one run. In terms of $Div_{Scenario}$, $DeepQTest_{TTC}$ significantly outperformed $DeepCollision$ on R1 and R2. On R3 and R4, $DeepQTest_{TTC}$ is either significantly better than or statistically equivalent to $DeepCollision$. The results of $Div_{Scenario}$ indicate that $DeepQTest_{TTC}$ might have more chance to test AVUT under more diverse test scenarios. Note that Div_{API} measures the diversity of applying environment configurations, while $Div_{Scenario}$ measures the diversity of test scenarios resulting from the environment configurations.

Conclusion for RQ3: $DeepQTest_{TTC}$ outperformed $DeepCollision$ in terms of *Realism Metrics* and *Diversity Metrics*. Concretely, as for *Realism Metrics*, $DeepQTest_{TTC}$ achieved a higher proportion of realistic scenarios among all the generated ones, and it also generated more realistic collision scenarios with less time. On the four roads under the four weather conditions, $DeepQTest_{TTC}$ identified on average 16 realistic collision scenarios out of 20 runs (i.e., $16/20=80\%$ per run), and it took on average 10.58 seconds to trigger a realistic collision scenario. In addition, $DeepQTest$ is effective in avoiding the generation of four kinds of unrealistic environment configurations. Regarding *Diversity Metrics*, $DeepQTest$ achieved an overall better performance than $DeepCollision$ in introducing diverse environment configurations (i.e., Div_{API}) and generating diverse scenarios (i.e., $Div_{Scenario}$).

6.4 Threats to Validity

Internal Validity. Threats to internal validity are concerned about the design factors that might have an impact on the conclusion. To migrate the potential threat to the internal validity caused by MDP formulation and DQN parameter settings, we trained the 12 $DeepQTest$ models following identical state encoding, action space, Q-network architecture, learning algorithm, training details, and hyperparameter settings, to ensure fair comparison among them. Another

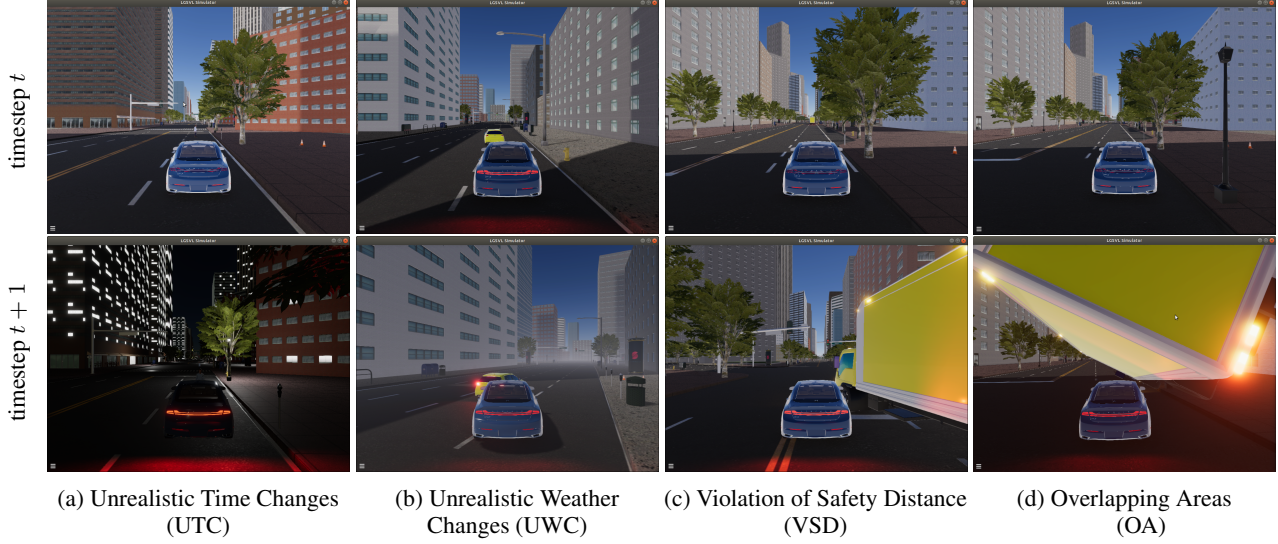


Figure 7: **Examples of Unrealistic Environment Configurations and the Resulting Unrealistic Driving Scenarios - RQ3.** From left to right are: (a) The AVUT was maintaining its lane and a pedestrian was standing on the sidewalk in front of the AVUT at timestep t , and at timestep $t + 1$, an environment configuration action changed the time from day to night and the AVUT collided with the pedestrian; (b) The AVUT and an NPC vehicle both were trying to change the left lane at timestep t , and at timestep $t + 1$, an environment configuration action that changed the weather condition to moderate fog was invoked, the invocation of the action caused a collision between the AVUT and the NPC vehicle; (c) The AVUT was maintaining its lane at timestep t , and at timestep $t + 1$, a truck was generated whose initial position violated the safety distance from the AVUT and caused a collision; (d) The AVUT was maintaining its lane at timestep t , and at timestep $t + 1$, a truck was generated whose area overlaps with the AVUT and directly caused a collision.

Table 9: Results of pair-wise comparisons of $DeepQTest_{TTC}$ and $DeepCollision$ in terms of *Diversity Metrics* using the Vargha and Delaney statistics and the Mann–Whitney U test - RQ3

	R1				R2				R3				R4			
	Div_{API}		$Div_{Scenario}$		Div_{API}		$Div_{Scenario}$		Div_{API}		$Div_{Scenario}$		Div_{API}		$Div_{Scenario}$	
$DeepQTest_{TTC}$ vs. $DeepCollision$	\hat{A}_{12}	p	\hat{A}_{12}	p	\hat{A}_{12}	p	\hat{A}_{12}	p	\hat{A}_{12}	p	\hat{A}_{12}	p	\hat{A}_{12}	p	\hat{A}_{12}	p
$DeepQTest_{TTC_{RD}}$	0.880	<0.05	0.909	<0.05	0.750	<0.05	0.739	<0.05	0.786	<0.05	0.767	<0.05	0.761	<0.05	0.570	0.455
$DeepQTest_{TTC_{RN}}$	0.839	<0.05	0.877	<0.05	0.730	<0.05	0.820	<0.05	0.774	<0.05	0.749	<0.05	0.838	<0.05	0.762	<0.05
$DeepQTest_{TTC_{SD}}$	0.870	<0.05	0.811	<0.05	0.805	<0.05	0.860	<0.05	0.785	<0.05	0.728	<0.05	0.719	<0.05	0.453	0.615
$DeepQTest_{TTC_{SN}}$	0.795	<0.05	0.844	<0.05	0.844	<0.05	0.799	<0.05	0.746	<0.05	0.679	0.054	0.765	<0.05	0.556	0.549

* R1: Road1; R2: Road2; R3: Road3; R4: Road4. RD: Rainy Day; RN: Rainy Night; SD: Sunny Day; SN: Sunny Night. p is p -value; a bold \hat{A}_{12} with a $p < 0.05$ implies that $DeepQTest$ is significantly better than $DeepCollision$, whereas a \hat{A}_{12} decorated by symbol "x" indicates $DeepQTest$ performed significantly worse than $DeepCollision$; a $p > 0.5$ means no significant difference between $DeepQTest$ and $DeepCollision$. \hat{A}_{12} magnitude: negligible ($\hat{A}_{12} \in (0.444, 0.556)$), small ($\hat{A}_{12} \in [0.556, 0.638)$ or $(0.362, 0.444]$), medium ($\hat{A}_{12} \in [0.638, 0.714)$ or $(0.286, 0.362]$), large ($\hat{A}_{12} \in [0.714, 1.0]$ or $[0, 0.286]$).

threat to internal validity is related to the potential faults within our algorithm infrastructure. To control this threat, we used the open-source machine learning framework, PyTorch [67], which has been widely applied and tested in both academics and industry. Furthermore, we realized that the hyperparameter tuning of DQN may have an influence on the performance of $DeepQTest$, therefore, we followed the default hyperparameter settings from Zhou [96] when training all of the 12 $DeepQTest$ models. We understand that tuning hyperparameters of DQN might improve the performance of $DeepQTest$, which unfortunately cannot be covered in this paper because it requires extensive and dedicated empirical studies.

External Validity. The threat is related to the currently applied subject system and simulator and the possible generalization to other case studies. In our evaluation, we conducted the empirical study with an industrial-scale ADS (i.e., Apollo) and a commonly applied simulator (i.e., LGSVL). We understand that conducting more case studies with different ADSs and simulators would help to better evaluate and generalize $DeepTest$, and using our already developed REST API endpoints, other ADSs, and simulators can be easily integrated with $DeepQTest$ with minimum effort. However, it is important to mention that experiments on testing ADSs in the simulation are very computationally expensive, which limited the number of case studies we used in our experiment.

Construct Validity. Threat to construct validity concerns whether the metrics for evaluation can precisely reflect the variables we want to measure in the experiment. As discussed in Section 5.4, we present three types of metrics (i.e., *Safety and Comfort Metrics*, *Realism Metrics*, and *Diversity Metrics*) including 16 comparable metrics (e.g., *TTC* and *#Collision*) to measure the effectiveness and efficiency of *DeepQTest*.

Conclusion Validity. The threat to conclusion validity is related to the use of appropriate analytical methods and the reliability of conclusions. To draw a reliable conclusion, we followed a rigorous procedure to collect the data and employed statistical methods to analyze the collected data. Specifically, 20 independent runs of each experiment setting were performed to account for randomness. In addition, following the guideline by Arcuri and Briand [5], we performed pairwise comparisons with the Mann-Whitney U test and used the Vargha-Delaney \hat{A}_{12} metric for effect size.

6.5 Data Availability

To enable the reproducibility of our research findings, we provide the replication package in our GitHub online repository⁴. The replication package contains the following contents: 1) all related algorithms and source code for conducting the experiment; 2) All the raw data for the experiment results and analyses; and 3) The REST API endpoints for configuring the environment.

7 Discussion

Recording and replaying scenarios for further diagnosis and analysis. Due to the complexity and uncertainty of the operating environment, as well as the complexity of the driving tasks, it is always very time-consuming to use simulations to evaluate scenarios of an ADS testing approach. Thus, it is necessary to record the generated scenarios to mitigate the cost for further possible analysis and usage. For example, the recorded scenarios could be utilized for supporting further diagnoses of ADSs, and can also be used for regression testing.

To facilitate the recording and reusing process of test scenarios, we first proposed a Domain-Specific Language (DSL) for scenario representation and evaluation, named *DeepScenario* [59], which is based on the *Driving Scenario* definition in Section 5. Additionally, to support automatically collecting and replaying driving scenarios when testing ADSs by *DeepQTest*, we developed an *ScenarioCollector* and an *ScenarioRunner* to easily collect and replay scenarios using *DeepQTest*. With *ScenarioCollector* and *DeepQTest*, driving scenarios that have been used for testing ADSs can be automatically recorded for further usage. Meanwhile, by selecting and replaying specific types of driving scenarios (e.g., collision scenarios) through *ScenarioRunner*, *DeepQTest* can better facilitate diagnoses of ADSs.

There are existing works in the literature that study scene representation and propose scene standards and support toolsets. For instance, GeoScenario [72] is an open DSL for autonomous driving scenario representation, and it has a toolset available that can support the design, evaluation, and execution of scenarios. ASAM OpenSCENARIO [65] is a file format for describing the dynamic content of driving and traffic simulators. Scenarios defined following the OpenSCENARIO standard can be executed by Carla ScenarioRunner [24]. Both specifications can be used for scenario representation and execution, however, the process of scenario definition requires a lot of manual work, which is time-consuming. *DeepQTest* automates both the scenario collection and execution process using *ScenarioCollector* and *ScenarioRunner*.

Finally, the recorded driving scenarios can also be used for regression testing of advanced ADS versions. Specifically, each scenario is associated with several attributes characterizing its execution results. By using search-based techniques (e.g., genetic algorithms), these associated attributes can support for selection and prioritizing of scenarios for regression testing of ADSs. The recorded driving scenarios and toolset for collecting and replaying these scenarios can be found in the replication package which is listed in Section 6.5.

Multi-objective DeepQTest. In the current design of *DeepQTest*, only one objective (i.e., reward) is used to guide the test scenarios generation process. In practice, however, multiple objectives are often considered due to the multi-objective nature of many sequential decision and adaptive optimization problems [57]. In addition, from the results of RQ2 in Section 6.2, correlations can be observed among the three selected reward functions, i.e., positive correlation between *TTC* and *DTO*, negative correlation between *TTC* (*DTO*) and *Jerk*. This observation inspires us to investigate different designs of *DeepQTest* which can optimize multi-objectives at one time. Considering that the selected rewards are to some extent interrelated, one possible solution can be deriving one objective by combining the multiple objectives together. However, if the considered objectives conflict with each other, and we want to achieve a trade-off between the conflicting objectives, then multi-objective reinforcement learning (MORL) can be utilized to find a policy that can

⁴<https://github.com/Simula-COMPLEX/DeepQTest>

optimize multiple objectives simultaneously [88]. We think that there is a need to provide a multi-objective strategy for *DeepQTest* in the future.

8 Conclusion and Future work

This paper proposed a reinforcement learning (RL)-based ADS testing approach, named *DeepQTest*, which adaptively learns critical configurations of the operating environment to generate test inputs for ADSs. *DeepQTest* employs Deep Q-Learning (DQN) as the RL solution and adopts three reward functions as the learning guidelines. To extract features from a high-dimensional operating environment, *DeepQTest* utilizes multi-modal sensor fusion as the state encoding. Furthermore, the environment configuration processes are realized through a list of REST API endpoints specifying which environment parameters will be configured and their values. In addition, the realism of the environment configurations is ensured with a list of predefined realistic constraints and the real-world effect generator, which maps real-world weather and time to simulation. To assess the cost-effectiveness of *DeepQTest*, we compared *DeepQTest* with three baselines, i.e., random, greedy, and a start-of-the-art RL-based approach namely *DeepCollision*. Results show that *DeepQTest* significantly outperformed random and greedy strategies in terms of all selected metrics. Compared to *DeepCollision*, *DeepQTest* is capable of generating more realistic scenarios leading to collisions for testing ADSs. We also compared different reward functions to study their performance, and *Time-To-Collision* achieved the overall best results that is set as a recommended reward function in *DeepQTest*.

In the future, we plan to study the generalization of *DeepQTest* with more case studies and conduct additional experiments on more ADSs and simulators. In addition, investigating algorithm settings and tuning hyperparameter settings is one of our future works. We plan to employ automatic hyperparameter optimization frameworks (e.g., Optuna [4] and Tune [56]) to facilitate this process. We also plan to study different RL solutions and the possibility of integrating these solutions with *DeepQTest*. Furthermore, environmental uncertainties are crucial factors for the safety and reliability of ADS, thus, systematically introducing and quantifying uncertainties in the operating environment is another future work. Finally, *DeepQTest* was evaluated with simulators and the generated driving scenarios tested ADS with the simulated vehicle in a simulated operating environment, while it is important to evaluate the effectiveness of generated scenarios in various testing contexts, e.g., hardware-in-the-loop and physical-world ADS testing. Studying the transferability of virtual testing to other ADS testing contexts is another work in the future.

ACKNOWLEDGMENTS

This work is supported by the Co-evolver project (No. 286898/F20) funded by the Research Council of Norway. Man Zhang is funded by the European Research Council (ERC) under the European Union’s Horizon 2020 research and innovation program (grant agreement No 864972).

References

- [1] Raja Ben Abdesslem, Shiva Nejati, Lionel C Briand, and Thomas Stifter. Testing vision-based control systems using learnable evolutionary algorithms. In *2018 IEEE/ACM 40th International Conference on Software Engineering (ICSE)*, pages 1016–1026. IEEE, 2018.
- [2] Raja Ben Abdesslem, Annibale Panichella, Shiva Nejati, Lionel C Briand, and Thomas Stifter. Testing autonomous cars for feature interaction failures using many-objective search. In *2018 33rd IEEE/ACM International Conference on Automated Software Engineering (ASE)*, pages 143–154. IEEE, 2018.
- [3] Sarder Fakhrol Abedin, Md Shirajum Munir, Nguyen H Tran, Zhu Han, and Choong Seon Hong. Data freshness and energy-efficient uav navigation optimization: A deep reinforcement learning approach. *IEEE Transactions on Intelligent Transportation Systems*, 2020.
- [4] Takuya Akiba, Shotaro Sano, Toshihiko Yanase, Takeru Ohta, and Masanori Koyama. Optuna: A next-generation hyperparameter optimization framework. In *Proceedings of the 25th ACM SIGKDD international conference on knowledge discovery & data mining*, pages 2623–2631, 2019.
- [5] Andrea Arcuri and Lionel Briand. A practical guide for using statistical tests to assess randomized algorithms in software engineering. In *2011 33rd International Conference on Software Engineering (ICSE)*, pages 1–10. IEEE, 2011.
- [6] Il Bae, Jaeyoung Moon, Junekyo Jung, H Suk, Taewoo Kim, Hyunbin Park, Jaekwang Cha, Jincheol Kim, Dohyun Kim, and Shiho Kim. Self-driving like a human driver instead of a robocar: Personalized comfortable driving experience for autonomous vehicles. *arXiv preprint arXiv:2001.03908*, 2020.

- [7] Francesco Bella and Roberta Russo. A collision warning system for rear-end collision: a driving simulator study. *Procedia-social and behavioral sciences*, 20:676–686, 2011.
- [8] Raja Ben Abdesslem, Shiva Nejati, Lionel C Briand, and Thomas Stifter. Testing advanced driver assistance systems using multi-objective search and neural networks. In *Proceedings of the 31st IEEE/ACM International Conference on Automated Software Engineering*, pages 63–74, 2016.
- [9] Mario Bijelic, Tobias Gruber, and Werner Ritter. Benchmarking image sensors under adverse weather conditions for autonomous driving. In *2018 IEEE Intelligent Vehicles Symposium (IV)*, pages 1773–1779. IEEE, 2018.
- [10] Paul E. Black. Ratcliff/obershelp pattern recognition. In *Dictionary of Algorithms and Data Structures [online]*. Available from: <https://www.nist.gov/dads/HTML/ratcliff0bershelp.html>, 2021.
- [11] Oliver Bühler and Joachim Wegener. Evolutionary functional testing. *Computers & Operations Research*, 35(10):3144–3160, 2008.
- [12] Alessandro Calò, Paolo Arcaini, Shaukat Ali, Florian Hauer, and Fuyuki Ishikawa. Generating avoidable collision scenarios for testing autonomous driving systems. In *2020 IEEE 13th International Conference on Software Testing, Validation and Verification (ICST)*, pages 375–386. IEEE, 2020.
- [13] Indra M Chakravarty, JD Roy, and Radha Govind Laha. Handbook of methods of applied statistics. 1967.
- [14] Baiming Chen, Xiang Chen, Qiong Wu, and Liang Li. Adversarial evaluation of autonomous vehicles in lane-change scenarios. *IEEE Transactions on Intelligent Transportation Systems*, 2021.
- [15] Jianyu Chen, Bodi Yuan, and Masayoshi Tomizuka. Model-free deep reinforcement learning for urban autonomous driving. In *2019 IEEE intelligent transportation systems conference (ITSC)*, pages 2765–2771. IEEE, 2019.
- [16] Long Chen, Xuemin Hu, Bo Tang, and Yu Cheng. Conditional dqn-based motion planning with fuzzy logic for autonomous driving. *IEEE Transactions on Intelligent Transportation Systems*, 2020.
- [17] Xiaozhi Chen, Huimin Ma, Ji Wan, Bo Li, and Tian Xia. Multi-view 3d object detection network for autonomous driving. In *Proceedings of the IEEE conference on Computer Vision and Pattern Recognition*, pages 1907–1915, 2017.
- [18] Felipe Codevilla, Antonio M Lopez, Vladlen Koltun, and Alexey Dosovitskiy. On offline evaluation of vision-based driving models. In *Proceedings of the European Conference on Computer Vision (ECCV)*, pages 236–251, 2018.
- [19] Felipe Codevilla, Matthias Müller, Antonio López, Vladlen Koltun, and Alexey Dosovitskiy. End-to-end driving via conditional imitation learning. In *2018 IEEE International Conference on Robotics and Automation (ICRA)*, pages 4693–4700. IEEE, 2018.
- [20] Anthony Corso, Peter Du, Katherine Driggs-Campbell, and Mykel J Kochenderfer. Adaptive stress testing with reward augmentation for autonomous vehicle validation. In *2019 IEEE Intelligent Transportation Systems Conference (ITSC)*, pages 163–168. IEEE, 2019.
- [21] Krzysztof Czarnecki. Operational world model ontology for automated driving systems—part 1: Road structure. *Waterloo Intelligent Systems Engineering Lab (WISE) Report, University of Waterloo*, 2018.
- [22] Shaveta Dargan, Munish Kumar, Maruthi Rohit Ayyagari, and Gulshan Kumar. A survey of deep learning and its applications: a new paradigm to machine learning. *Archives of Computational Methods in Engineering*, 27(4):1071–1092, 2020.
- [23] Kalyanmoy Deb, Amrit Pratap, Sameer Agarwal, and TAMT Meyarivan. A fast and elitist multiobjective genetic algorithm: Nsga-ii. *IEEE transactions on evolutionary computation*, 6(2):182–197, 2002.
- [24] Alexey Dosovitskiy, German Ros, Felipe Codevilla, Antonio Lopez, and Vladlen Koltun. Carla: An open urban driving simulator. In *Conference on robot learning*, pages 1–16. PMLR, 2017.
- [25] Gabriel Dulac-Arnold, Richard Evans, Hado van Hasselt, Peter Sunehag, Timothy Lillicrap, Jonathan Hunt, Timothy Mann, Theophane Weber, Thomas Degris, and Ben Coppin. Deep reinforcement learning in large discrete action spaces. *arXiv preprint arXiv:1512.07679*, 2015.
- [26] Gabriel Dulac-Arnold, Daniel Mankowitz, and Todd Hester. Challenges of real-world reinforcement learning. *arXiv preprint arXiv:1904.12901*, 2019.
- [27] Haoyang Fan, Fan Zhu, Changchun Liu, Liangliang Zhang, Li Zhuang, Dong Li, Weicheng Zhu, Jiangtao Hu, Hongye Li, and Qi Kong. Baidu apollo em motion planner. *arXiv preprint arXiv:1807.08048*, 2018.
- [28] Di Feng, Christian Haase-Schütz, Lars Rosenbaum, Heinz Hertlein, Claudius Glaeser, Fabian Timm, Werner Wiesbeck, and Klaus Dietmayer. Deep multi-modal object detection and semantic segmentation for autonomous driving: Datasets, methods, and challenges. *IEEE Transactions on Intelligent Transportation Systems*, 22(3):1341–1360, 2020.

- [29] Settimio Ferlisi, Antonio Marchese, and Dario Peduto. Quantitative analysis of the risk to road networks exposed to slow-moving landslides: a case study in the campania region (southern italy). *Landslides*, 18:303–319, 2021.
- [30] Andrei Furda and Ljubo Vlacic. Enabling safe autonomous driving in real-world city traffic using multiple criteria decision making. *IEEE Intelligent Transportation Systems Magazine*, 3(1):4–17, 2011.
- [31] Des Greer and Guenther Ruhe. Software release planning: an evolutionary and iterative approach. *Information and software technology*, 46(4):243–253, 2004.
- [32] Jianmin Guo, Yu Jiang, Yue Zhao, Quan Chen, and Jiaguang Sun. Dlfuzz: Differential fuzzing testing of deep learning systems. In *Proceedings of the 2018 26th ACM Joint Meeting on European Software Engineering Conference and Symposium on the Foundations of Software Engineering*, pages 739–743, 2018.
- [33] Junyao Guo, Unmesh Kurup, and Mohak Shah. Is it safe to drive? an overview of factors, metrics, and datasets for driveability assessment in autonomous driving. *IEEE Transactions on Intelligent Transportation Systems*, 21(8):3135–3151, 2019.
- [34] Qishen Ha, Kohei Watanabe, Takumi Karasawa, Yoshitaka Ushiku, and Tatsuya Harada. Mfnet: Towards real-time semantic segmentation for autonomous vehicles with multi-spectral scenes. In *2017 IEEE/RSJ International Conference on Intelligent Robots and Systems (IROS)*, pages 5108–5115. IEEE, 2017.
- [35] Fitash Ul Haq, Donghwan Shin, and Lionel Briand. Many-objective reinforcement learning for online testing of dnn-enabled systems. *arXiv preprint arXiv:2210.15432*, 2022.
- [36] Fitash Ul Haq, Donghwan Shin, Shiva Nejati, and Lionel C Briand. Comparing offline and online testing of deep neural networks: An autonomous car case study. In *2020 IEEE 13th International Conference on Software Testing, Validation and Verification (ICST)*, pages 85–95. IEEE, 2020.
- [37] Fabrice Harel-Canada, Lingxiao Wang, Muhammad Ali Gulzar, Quanquan Gu, and Miryung Kim. Is neuron coverage a meaningful measure for testing deep neural networks? In *Proceedings of the 28th ACM Joint Meeting on European Software Engineering Conference and Symposium on the Foundations of Software Engineering*, pages 851–862, 2020.
- [38] Mark Harman, Phil McMinn, Jerffeson Teixeira de Souza, and Shin Yoo. Search based software engineering: Techniques, taxonomy, tutorial. In *Empirical software engineering and verification*, pages 1–59. Springer, 2010.
- [39] Sepp Hochreiter and Jürgen Schmidhuber. Long short-term memory. *Neural computation*, 9(8):1735–1780, 1997.
- [40] Qiang Hu, Lei Ma, Xiaofei Xie, Bing Yu, Yang Liu, and Jianjun Zhao. Deepmutation++: A mutation testing framework for deep learning systems. In *2019 34th IEEE/ACM International Conference on Automated Software Engineering (ASE)*, pages 1158–1161. IEEE, 2019.
- [41] Teemu H Itkonen, Jami Pekkanen, Otto Lappi, Iisakki Kosonen, Tapio Luttinen, and Heikki Summala. Trade-off between jerk and time headway as an indicator of driving style. *PloS one*, 12(10):e0185856, 2017.
- [42] Yaochu Jin. Surrogate-assisted evolutionary computation: Recent advances and future challenges. *Swarm and Evolutionary Computation*, 1(2):61–70, 2011.
- [43] Shinpei Kato, Shota Tokunaga, Yuya Maruyama, Seiya Maeda, Manato Hirabayashi, Yuki Kitsukawa, Abraham Monroy, Tomohito Ando, Yusuke Fujii, and Takuya Azumi. Autoware on board: Enabling autonomous vehicles with embedded systems. In *2018 ACM/IEEE 9th International Conference on Cyber-Physical Systems (ICCPs)*, pages 287–296. IEEE, 2018.
- [44] Christoph G Keller and Dariu M Gavrilă. Will the pedestrian cross? a study on pedestrian path prediction. *IEEE Transactions on Intelligent Transportation Systems*, 15(2):494–506, 2013.
- [45] Jinhan Kim, Robert Feldt, and Shin Yoo. Guiding deep learning system testing using surprise adequacy. In *2019 IEEE/ACM 41st International Conference on Software Engineering (ICSE)*, pages 1039–1049. IEEE, 2019.
- [46] B Ravi Kiran, Ibrahim Sobh, Victor Talpaert, Patrick Mannion, Ahmad A Al Sallab, Senthil Yogamani, and Patrick Pérez. Deep reinforcement learning for autonomous driving: A survey. *IEEE Transactions on Intelligent Transportation Systems*, 2021.
- [47] B Ravi Kiran, Ibrahim Sobh, Victor Talpaert, Patrick Mannion, Ahmad A Al Sallab, Senthil Yogamani, and Patrick Pérez. Deep reinforcement learning for autonomous driving: A survey. *arXiv preprint arXiv:2002.00444*, 2020.
- [48] Barbara Kitchenham, Lech Madeyski, David Budgen, Jacky Keung, Pearl Brereton, Stuart Charters, Shirley Gibbs, and Amnart Pohthong. Robust statistical methods for empirical software engineering. *Empirical Software Engineering*, 22(2):579–630, 2017.
- [49] Mykel J. Kochenderfer and Kyle H. Wray Tim A. Wheeler. *Algorithms for Decision Making*. MIT press, 2022.

- [50] Maxim Kolchin and Fedor Kozlov. A template-based information extraction from web sites with unstable markup. In *Semantic Web Evaluation Challenge: SemWebEval 2014 at ESWC 2014, Anissaras, Crete, Greece, May 25-29, 2014, Revised Selected Papers*, pages 89–94. Springer, 2014.
- [51] Abdullah Konak, David W Coit, and Alice E Smith. Multi-objective optimization using genetic algorithms: A tutorial. *Reliability engineering & system safety*, 91(9):992–1007, 2006.
- [52] Peter Koonce and Lee Rodegerdts. Traffic signal timing manual. Technical report, United States. Federal Highway Administration, 2008.
- [53] Alex Krizhevsky, Ilya Sutskever, and Geoffrey E Hinton. Imagenet classification with deep convolutional neural networks. *Advances in neural information processing systems*, 25:1097–1105, 2012.
- [54] Bo Li, Tianlei Zhang, and Tian Xia. Vehicle detection from 3d lidar using fully convolutional network. *arXiv preprint arXiv:1608.07916*, 2016.
- [55] Guanpeng Li, Yiran Li, Saurabh Jha, Timothy Tsai, Michael Sullivan, Siva Kumar Sastry Hari, Zbigniew Kalbarczyk, and Ravishankar Iyer. Av-fuzzer: Finding safety violations in autonomous driving systems. In *2020 IEEE 31st International Symposium on Software Reliability Engineering (ISSRE)*, pages 25–36. IEEE, 2020.
- [56] Richard Liaw, Eric Liang, Robert Nishihara, Philipp Moritz, Joseph E Gonzalez, and Ion Stoica. Tune: A research platform for distributed model selection and training. *arXiv preprint arXiv:1807.05118*, 2018.
- [57] Chunming Liu, Xin Xu, and Dewen Hu. Multiobjective reinforcement learning: A comprehensive overview. *IEEE Transactions on Systems, Man, and Cybernetics: Systems*, 45(3):385–398, 2014.
- [58] Chengjie Lu, Yize Shi, Huihui Zhang, Man Zhang, Tiexin Wang, Tao Yue, and Shaukat Ali. Learning configurations of operating environment of autonomous vehicles to maximize their collisions. *IEEE Transactions on Software Engineering*, 49(1):384–402, 2022.
- [59] Chengjie Lu, Tao Yue, and Shaukat Ali. Deepscenario: An open driving scenario dataset for autonomous driving system testing. In *2023 IEEE/ACM 20th International Conference on Mining Software Repositories (MSR)*, pages 52–56, 2023.
- [60] Lei Ma, Fuyuan Zhang, Jiyuan Sun, Minhui Xue, Bo Li, Felix Juefei-Xu, Chao Xie, Li Li, Yang Liu, Jianjun Zhao, et al. Deepmutation: Mutation testing of deep learning systems. In *2018 IEEE 29th International Symposium on Software Reliability Engineering (ISSRE)*, pages 100–111. IEEE, 2018.
- [61] Hiroya Maeda, Yoshihide Sekimoto, Toshikazu Seto, Takehiro Kashiyama, and Hiroshi Omata. Road damage detection using deep neural networks with images captured through a smartphone. *arXiv preprint arXiv:1801.09454*, 2018.
- [62] Henry B Mann and Donald R Whitney. On a test of whether one of two random variables is stochastically larger than the other. *The annals of mathematical statistics*, pages 50–60, 1947.
- [63] Volodymyr Mnih, Koray Kavukcuoglu, David Silver, Andrei A Rusu, Joel Veness, Marc G Bellemare, Alex Graves, Martin Riedmiller, Andreas K Fidjeland, Georg Ostrovski, et al. Human-level control through deep reinforcement learning. *nature*, 518(7540):529–533, 2015.
- [64] Mustafa Mukadam, Akansel Cosgun, Alireza Nakhaei, and Kikuo Fujimura. Tactical decision making for lane changing with deep reinforcement learning. 2017.
- [65] American Society of Addiction Medicine. Asam openscenario, 2022.
- [66] OMG. Object constraint language v2.0. Object Management Group Adopted Specification (formal/06-05-01), 2006.
- [67] Adam Paszke, Sam Gross, Francisco Massa, Adam Lerer, James Bradbury, Gregory Chanan, Trevor Killeen, Zeming Lin, Natalia Gimelshein, Luca Antiga, et al. Pytorch: An imperative style, high-performance deep learning library. *Advances in neural information processing systems*, 32:8026–8037, 2019.
- [68] Kexin Pei, Yinzhi Cao, Junfeng Yang, and Suman Jana. Deepxplore: Automated whitebox testing of deep learning systems. In *proceedings of the 26th Symposium on Operating Systems Principles*, pages 1–18, 2017.
- [69] Zi Peng, Jinqiu Yang, Tse-Hsun Chen, and Lei Ma. A first look at the integration of machine learning models in complex autonomous driving systems: a case study on apollo. In *Proceedings of the 28th ACM Joint Meeting on European Software Engineering Conference and Symposium on the Foundations of Software Engineering*, pages 1240–1250, 2020.
- [70] Andreas Pfeuffer and Klaus Dietmayer. Optimal sensor data fusion architecture for object detection in adverse weather conditions. In *2018 21st International Conference on Information Fusion (FUSION)*, pages 1–8. IEEE, 2018.

- [71] Florian Piewak, Peter Pinggera, Markus Enzweiler, David Pfeiffer, and Marius Zöllner. Improved semantic stixels via multimodal sensor fusion. In *German Conference on Pattern Recognition*, pages 447–458. Springer, 2018.
- [72] Rodrigo Queiroz, Thorsten Berger, and Krzysztof Czarnecki. Geoscenario: An open dsl for autonomous driving scenario representation. In *2019 IEEE Intelligent Vehicles Symposium (IV)*, pages 287–294. IEEE, 2019.
- [73] Jin Woo Ro, Partha S Roop, and Avinash Malik. A new safety distance calculation for rear-end collision avoidance. *IEEE Transactions on Intelligent Transportation Systems*, 22(3):1742–1747, 2020.
- [74] Carlos Rodríguez, Marcos Baez, Florian Daniel, Fabio Casati, Juan Carlos Trabucco, Luigi Canali, and Gianraffaele Percannella. Rest apis: a large-scale analysis of compliance with principles and best practices. In *International conference on web engineering*, pages 21–39. Springer, 2016.
- [75] Guodong Rong, Byung Hyun Shin, Hadi Tabatabaee, Qiang Lu, Steve Lemke, Mārtinš Možeiko, Eric Boise, Geehoon Uhm, Mark Gerow, Shalin Mehta, et al. Lgsvl simulator: A high fidelity simulator for autonomous driving. In *2020 IEEE 23rd International Conference on Intelligent Transportation Systems (ITSC)*, pages 1–6. IEEE, 2020.
- [76] Zhang Ruiming, Liu Chengju, and Chen Qijun. End-to-end control of kart agent with deep reinforcement learning. In *2018 IEEE International Conference on Robotics and Biomimetics (ROBIO)*, pages 1688–1693. IEEE, 2018.
- [77] Ahmad EL Sallab, Mohammed Abdou, Etienne Perot, and Senthil Yogamani. Deep reinforcement learning framework for autonomous driving. *Electronic Imaging*, 2017(19):70–76, 2017.
- [78] Lukas Schneider, Manuel Jasch, Björn Fröhlich, Thomas Weber, Uwe Franke, Marc Pollefeys, and Matthias Rätzsch. Multimodal neural networks: Rgb-d for semantic segmentation and object detection. In *Scandinavian conference on image analysis*, pages 98–109. Springer, 2017.
- [79] Adnan Shaout, Dominic Colella, and Selim Awad. Advanced driver assistance systems-past, present and future. In *2011 Seventh International Computer Engineering Conference (ICENCO'2011)*, pages 72–82. IEEE, 2011.
- [80] Jana Sillmann, Thordis Thorarinsdottir, Noel Keenlyside, Nathalie Schaller, Lisa V Alexander, Gabriele Hegerl, Sonia I Seneviratne, Robert Vautard, Xuebin Zhang, and Francis W Zwiers. Understanding, modeling and predicting weather and climate extremes: Challenges and opportunities. *Weather and climate extremes*, 18:65–74, 2017.
- [81] Karen Simonyan and Andrew Zisserman. Very deep convolutional networks for large-scale image recognition. *arXiv preprint arXiv:1409.1556*, 2014.
- [82] Jonathan Kelly Steven-Waslander. Motion planning for self-driving cars. *Coursera&University of Toronto*, <https://www.coursera.org/lecture/motion-planning-self-driving-cars/lesson-3-time-to-collision-pS9zI>, 2021.
- [83] Andrea Stocco, Brian Pulfer, and Paolo Tonella. Mind the gap! a study on the transferability of virtual vs physical-world testing of autonomous driving systems. *IEEE Transactions on Software Engineering*, 2022.
- [84] Richard S Sutton and Andrew G Barto. *Reinforcement learning: An introduction*. MIT press, 2018.
- [85] Baidu Apollo team. Apollo: Open source autonomous driving, 2017.
- [86] Yuchi Tian, Kexin Pei, Suman Jana, and Baishakhi Ray. Deeptest: Automated testing of deep-neural-network-driven autonomous cars. In *Proceedings of the 40th international conference on software engineering*, pages 303–314, 2018.
- [87] Simon Ulbrich, Till Menzel, Andreas Reschka, Fabian Schuldt, and Markus Maurer. Defining and substantiating the terms scene, situation, and scenario for automated driving. In *2015 IEEE 18th International Conference on Intelligent Transportation Systems*, pages 982–988. IEEE, 2015.
- [88] Peter Vamplew, Richard Dazeley, Adam Berry, Rustam Issabekov, and Evan Dekker. Empirical evaluation methods for multiobjective reinforcement learning algorithms. 2011.
- [89] Harsha Vardhan. Hd maps: New age maps powering autonomous vehicles. *Geospatial world*, 22, 2017.
- [90] Katja Vogel. A comparison of headway and time to collision as safety indicators. *Accident analysis & prevention*, 35(3):427–433, 2003.
- [91] Christopher JCH Watkins and Peter Dayan. Q-learning. *Machine learning*, 8(3-4):279–292, 1992.
- [92] Xiaofei Xie, Lei Ma, Felix Juefei-Xu, Minhui Xue, Hongxu Chen, Yang Liu, Jianjun Zhao, Bo Li, Jianxiong Yin, and Simon See. Deephunter: A coverage-guided fuzz testing framework for deep neural networks. In *Proceedings of the 28th ACM SIGSOFT International Symposium on Software Testing and Analysis*, pages 146–157, 2019.
- [93] Mengshi Zhang, Yuqun Zhang, Lingming Zhang, Cong Liu, and Sarfraz Khurshid. Deeproad: Gan-based metamorphic testing and input validation framework for autonomous driving systems. In *2018 33rd IEEE/ACM International Conference on Automated Software Engineering (ASE)*, pages 132–142. IEEE, 2018.

-
- [94] Zijun Zhang. Improved adam optimizer for deep neural networks. In *2018 IEEE/ACM 26th International Symposium on Quality of Service (IWQoS)*, pages 1–2. IEEE, 2018.
- [95] Husheng Zhou, Wei Li, Zelun Kong, Junfeng Guo, Yuqun Zhang, Bei Yu, Lingming Zhang, and Cong Liu. Deepbillboard: Systematic physical-world testing of autonomous driving systems. In *Proceedings of the ACM/IEEE 42nd International Conference on Software Engineering*, pages 347–358, 2020.
- [96] Morvan Zhou. pytorch tutorials. <https://github.com/MorvanZhou/PyTorch-Tutorial>, 2021.
- [97] Wei Zhou, Julie Stephany Berrio, Stewart Worrall, and Eduardo Nebot. Automated evaluation of semantic segmentation robustness for autonomous driving. *IEEE Transactions on Intelligent Transportation Systems*, 21(5):1951–1963, 2019.
- [98] Meixin Zhu, Yinhai Wang, Ziyuan Pu, Jingyun Hu, Xuesong Wang, and Ruimin Ke. Safe, efficient, and comfortable velocity control based on reinforcement learning for autonomous driving. *Transportation Research Part C: Emerging Technologies*, 117:102662, 2020.

Appendix

Algorithm 4 Pseudo-Code of *DeepQTest* Environment Configuration Learning

Input

Let $TEnv$ be the test environment; AS be the environment configuration action space; $terminate$ be the stopping criteria.

Output

Act_{list} : a list of actions selected from AS

```

1:  $Act_{list} \leftarrow []$ 
2: Initialize replay memory  $D$  with capacity  $N$ ; Initialize Q-network  $Q$  with random weights  $\theta$ ; Initialize target network  $\hat{Q}$  with weights  $\theta^- = \theta$ 
3: for episode = 1,  $M$  do
4:    $s_t \leftarrow$  observe a state of  $TEnv$ 
5:   while  $\neg terminate$  do
6:      $act_t = \begin{cases} \arg \max_a Q(s_t, a), & \text{with probability } 1-\epsilon \\ \text{randomly select an action,} & \epsilon \end{cases}$ 
7:      $terminate, r_t, s_{t+1} \leftarrow \text{step}(act_t, s_t)$ 
8:     Store transition  $\langle s_t, a_t, r_t, s_{t+1} \rangle$  in  $D$ 
9:     if  $D$  is full then
10:       Sample random minibatch of transition  $\langle s_t, a_t, r_t, s_{t+1} \rangle$  from  $D$ 
11:       Update Q-network
12:     end if
13:     Every  $C$  steps reset  $\hat{Q} = Q$ 
14:      $s_t \leftarrow s_{t+1}$ 
15:     Put  $act_t$  into  $Act_{list}$ 
16:   end while
17: end for
18: return  $Act_{list}$ 

```

Algorithm 5 Pseudo-Code of Scenario Similarity Calculation**Input**

Let $S_a = \langle scene_a^1, scene_a^2, \dots, scene_a^n \rangle$, $S_b = \langle scene_b^1, scene_b^2, \dots, scene_b^n \rangle$ be two driving scenarios;
 A scene is defined as $scene = \langle property^1, property^2, \dots, property^{np} \rangle$;

Output

$similarity_{scenario}$: similarity between S_a and S_b .

```

1: function SCENARIOSIMILARITY( $S_a, S_b$ )
2:    $similarity_{scenario} \leftarrow 0$ 
3:   for  $interval \leftarrow 0$  to  $n - 1$  do
4:      $similarity_{ab}, similarity_{ba} \leftarrow 0, 0$ 
5:     for  $i \leftarrow 1$  to  $n - interval$  do
6:        $similarity_{ab} \leftarrow similarity_{ab} + SCENESIMILARITY(scene_a^i, scene_b^{i+interval})$ 
7:        $similarity_{ba} \leftarrow similarity_{ba} + SCENESIMILARITY(scene_b^i, scene_a^{i+interval})$ 
8:     end for
9:      $similarity_{scenario} \leftarrow \max \{similarity_{scenario}, similarity_{ab}/n, similarity_{ba}/n\}$ 
10:  end for
11:  return  $similarity_{scenario}$ 
12: end function

13: function SCENESIMILARITY( $scene_a, scene_b$ )
14:    $similarity_{scene} \leftarrow 0$ 
15:   for  $i \leftarrow 1$  to  $np$  do
16:     if  $property_a^i \notin Obstacles$  then                                 $\triangleright Obstacles$  is  $\{NPCVehicles, Pedestrians, StaticObstacles\}$ 
17:       if  $property_a^i = property_b^i$  then
18:          $similarity_{scene} \leftarrow similarity_{scene} + 1$ 
19:       else
20:          $similarity_{scene} \leftarrow similarity_{scene} + OBSTACLESIMILARITY(property_a^i, property_b^i)$ 
21:       end if
22:     end if
23:   end for
24:   return  $similarity_{scene}/np$ 
25: end function

26: function OBSTACLESIMILARITY( $obstacles_a, obstacles_b$ )
27:    $similarity \leftarrow 0$ 
28:    $number_a, number_b = COUNTOBSTACLES(obstacles_a), COUNTOBSTACLES(obstacles_b)$ 
29:    $outer_{obstacles}, inner_{obstacles} \leftarrow obstacles_a, obstacles_b$ 
30:   if  $number_a \leq number_b$  then
31:      $outer_{obstacles}, inner_{obstacles} \leftarrow obstacles_b, obstacles_a$ 
32:   end if
33:   for  $i \leftarrow 1$  to  $\min\{number_a, number_b\}$  do
34:      $similarity_i \leftarrow 0$ 
35:     for  $j \leftarrow 1$  to  $\max\{number_a, number_b\}$  do
36:        $similarity_i \leftarrow \max\{similarity_i, COUNTIDENTICALVALUES(outer_{obstacles}(i), inner_{obstacles}(j))\}$ 
37:     end for
38:      $similarity \leftarrow similarity + similarity_i$ 
39:   end for
40:   return  $similarity / (number_a + number_b)$ 
41: end function

```

Table 10: Results of the Vargha and Delaney statistics and the Mann–Whitney U test (TTC_{Reward}) - RQ1

<i>DeepQTest</i> vs. (<i>RS</i> , <i>GS</i>)		<i>TTC</i>		<i>DTO</i>		<i>Jerk</i>		<i>#Collision</i>		<i>CollisionTime</i>	
		\hat{A}_{12}	<i>p</i>	\hat{A}_{12}	<i>p</i>	\hat{A}_{12}	<i>p</i>	\hat{A}_{12}	<i>p</i>	\hat{A}_{12}	<i>p</i>
<i>DeepQTestTTC_{RD}</i>											
<i>R1</i>	<i>RS</i>	0.117	<0.05	0.090	<0.05	0.820	<0.05	0.825	<0.05	0.155	<0.05
	<i>GS</i>	0.058	<0.05	0.168	<0.05	0.795	<0.05	0.825	<0.05	0.233	<0.05
<i>R2</i>	<i>RS</i>	0.133	<0.05	0.117	<0.05	0.713	<0.05	0.775	<0.05	0.190	<0.05
	<i>GS</i>	0.195	<0.05	0.138	<0.05	0.716	<0.05	0.700	<0.05	0.226	<0.05
<i>R3</i>	<i>RS</i>	0.158	<0.05	0.155	<0.05	0.552	0.579	0.750	<0.05	0.228	<0.05
	<i>GS</i>	0.160	<0.05	0.128	<0.05	0.535	0.715	0.675	<0.05	0.270	<0.05
<i>R4</i>	<i>RS</i>	0.005	<0.05	0.113	<0.05	0.895	<0.05	0.900	<0.05	0.109	<0.05
	<i>GS</i>	0.010	<0.05	0.068	<0.05	0.848	<0.05	0.900	<0.05	0.090	<0.05
<i>DeepQTestTTC_{RN}</i>											
<i>R1</i>	<i>RS</i>	0.075	<0.05	0.045	<0.05	0.897	<0.05	0.900	<0.05	0.100	<0.05
	<i>GS</i>	0.043	<0.05	0.087	<0.05	0.843	<0.05	0.775	<0.05	0.185	<0.05
<i>R2</i>	<i>RS</i>	0.170	<0.05	0.070	<0.05	0.698	<0.05	0.850	<0.05	0.131	<0.05
	<i>GS</i>	0.107	<0.05	0.052	<0.05	0.748	<0.05	0.750	<0.05	0.119	<0.05
<i>R3</i>	<i>RS</i>	0.068	<0.05	0.152	<0.05	0.618	0.208	0.725	<0.05	0.241	<0.05
	<i>GS</i>	0.087	<0.05	0.085	<0.05	0.512	0.903	0.625	0.122	0.316	<0.05
<i>R4</i>	<i>RS</i>	0.072	<0.05	0.043	<0.05	0.848	<0.05	0.800	<0.05	0.203	<0.05
	<i>GS</i>	0.077	<0.05	0.068	<0.05	0.840	<0.05	0.850	<0.05	0.134	<0.05
<i>DeepQTestTTC_{SD}</i>											
<i>R1</i>	<i>RS</i>	0.045	<0.05	0.165	<0.05	0.860	<0.05	0.850	<0.05	0.111	<0.05
	<i>GS</i>	0.092	<0.05	0.185	<0.05	0.833	<0.05	0.825	<0.05	0.150	<0.05
<i>R2</i>	<i>RS</i>	0.102	<0.05	0.070	<0.05	0.637	0.140	0.775	<0.05	0.188	<0.05
	<i>GS</i>	0.070	<0.05	0.098	<0.05	0.652	0.102	0.775	<0.05	0.206	<0.05
<i>R3</i>	<i>RS</i>	0.163	<0.05	0.050	<0.05	0.610	0.239	0.850	<0.05	0.126	<0.05
	<i>GS</i>	0.195	<0.05	0.092	<0.05	0.557	0.543	0.775	<0.05	0.150	<0.05
<i>R4</i>	<i>RS</i>	0.025	<0.05	0.052	<0.05	0.868	<0.05	0.925	<0.05	0.075	<0.05
	<i>GS</i>	0.077	<0.05	0.055	<0.05	0.802	<0.05	0.800	<0.05	0.121	<0.05
<i>DeepQTestTTC_{SN}</i>											
<i>R1</i>	<i>RS</i>	0.035	<0.05	0.175	<0.05	0.757	<0.05	0.900	<0.05	0.084	<0.05
	<i>GS</i>	0.048	<0.05	0.158	<0.05	0.740	<0.05	0.900	<0.05	0.084	<0.05
<i>R2</i>	<i>RS</i>	0.045	<0.05	0.010	<0.05	0.630	0.164	0.825	<0.05	0.151	<0.05
	<i>GS</i>	0.058	<0.05	0.102	<0.05	0.740	<0.05	0.800	<0.05	0.163	<0.05
<i>R3</i>	<i>RS</i>	0.270	<0.05	0.102	<0.05	0.718	<0.05	0.825	<0.05	0.139	<0.05
	<i>GS</i>	0.098	<0.05	0.122	<0.05	0.650	0.107	0.700	<0.05	0.287	<0.05
<i>R4</i>	<i>RS</i>	0.035	<0.05	0.052	<0.05	0.815	<0.05	0.875	<0.05	0.138	<0.05
	<i>GS</i>	0.052	<0.05	0.058	<0.05	0.748	<0.05	0.875	<0.05	0.138	<0.05

Table 11: Results of the Vargha and Delaney statistics and the Mann–Whitney U test (DTO_{Reward}) - RQ1

<i>DeepQTest</i> vs. (<i>RS</i> , <i>GS</i>)		<i>TTC</i>		<i>DTO</i>		<i>Jerk</i>		<i>#Collision</i>		<i>CollisionTime</i>	
		\hat{A}_{12}	<i>p</i>	\hat{A}_{12}	<i>p</i>	\hat{A}_{12}	<i>p</i>	\hat{A}_{12}	<i>p</i>	\hat{A}_{12}	<i>p</i>
<i>DeepQTest</i> _{<i>DTOR</i><i>D</i>}											
<i>R1</i>	<i>RS</i>	0.198	<0.05	0.055	<0.05	0.713	<0.05	0.750	<0.05	0.203	<0.05
	<i>GS</i>	0.098	<0.05	0.060	<0.05	0.719	<0.05	0.825	<0.05	0.158	<0.05
<i>R2</i>	<i>RS</i>	0.133	<0.05	0.072	<0.05	0.540	0.675	0.850	<0.05	0.083	<0.05
	<i>GS</i>	0.085	<0.05	0.058	<0.05	0.675	0.060	0.875	<0.05	0.095	<0.05
<i>R3</i>	<i>RS</i>	0.170	<0.05	0.075	<0.05	0.502	0.989	0.575	0.356	0.340	0.063
	<i>GS</i>	0.163	<0.05	0.068	<0.05	0.547	0.617	0.700	<0.05	0.287	<0.05
<i>R4</i>	<i>RS</i>	0.212	<0.05	0.075	<0.05	0.823	<0.05	0.750	<0.05	0.229	<0.05
	<i>GS</i>	0.268	<0.05	0.065	<0.05	0.858	<0.05	0.825	<0.05	0.175	<0.05
<i>DeepQTest</i> _{<i>DTOR</i><i>N</i>}											
<i>R1</i>	<i>RS</i>	0.125	<0.05	0.055	<0.05	0.685	<0.05	0.875	<0.05	0.105	<0.05
	<i>GS</i>	0.130	<0.05	0.080	<0.05	0.665	0.076	0.875	<0.05	0.107	<0.05
<i>R2</i>	<i>RS</i>	0.080	<0.05	0.060	<0.05	0.455	0.636	0.775	<0.05	0.161	<0.05
	<i>GS</i>	0.115	<0.05	0.055	<0.05	0.497	0.989	0.800	<0.05	0.163	<0.05
<i>R3</i>	<i>RS</i>	0.147	<0.05	0.010	<0.05	0.748	<0.05	0.850	<0.05	0.135	<0.05
	<i>GS</i>	0.150	<0.05	0.018	<0.05	0.770	<0.05	0.775	<0.05	0.171	<0.05
<i>R4</i>	<i>RS</i>	0.282	<0.05	0.010	<0.05	0.850	<0.05	0.900	<0.05	0.085	<0.05
	<i>GS</i>	0.328	<0.05	0.033	<0.05	0.772	<0.05	0.875	<0.05	0.087	<0.05
<i>DeepQTest</i> _{<i>DTOS</i><i>D</i>}											
<i>R1</i>	<i>RS</i>	0.168	<0.05	0.043	<0.05	0.723	<0.05	0.750	<0.05	0.261	<0.05
	<i>GS</i>	0.160	<0.05	0.040	<0.05	0.723	<0.05	0.675	<0.05	0.254	<0.05
<i>R2</i>	<i>RS</i>	0.048	<0.05	0.068	<0.05	0.378	0.190	0.825	<0.05	0.099	<0.05
	<i>GS</i>	0.087	<0.05	0.080	<0.05	0.438	0.508	0.850	<0.05	0.109	<0.05
<i>R3</i>	<i>RS</i>	0.100	<0.05	0.048	<0.05	0.730	<0.05	0.800	<0.05	0.158	<0.05
	<i>GS</i>	0.145	<0.05	0.055	<0.05	0.698	<0.05	0.750	<0.05	0.209	<0.05
<i>R4</i>	<i>RS</i>	0.282	<0.05	0.055	<0.05	0.830	<0.05	0.825	<0.05	0.144	<0.05
	<i>GS</i>	0.388	0.059	0.065	<0.05	0.828	<0.05	0.800	<0.05	0.179	<0.05
<i>DeepQTest</i> _{<i>DTOS</i><i>N</i>}											
<i>R1</i>	<i>RS</i>	0.233	<0.05	0.070	<0.05	0.797	<0.05	0.825	<0.05	0.168	<0.05
	<i>GS</i>	0.278	<0.05	0.045	<0.05	0.834	<0.05	0.725	<0.05	0.259	<0.05
<i>R2</i>	<i>RS</i>	0.193	<0.05	0.090	<0.05	0.398	0.273	0.825	<0.05	0.130	<0.05
	<i>GS</i>	0.165	<0.05	0.090	<0.05	0.470	0.756	0.775	<0.05	0.269	<0.05
<i>R3</i>	<i>RS</i>	0.102	<0.05	0.037	<0.05	0.490	0.925	0.800	<0.05	0.142	<0.05
	<i>GS</i>	0.105	<0.05	0.025	<0.05	0.472	0.776	0.800	<0.05	0.138	<0.05
<i>R4</i>	<i>RS</i>	0.228	<0.05	0.035	<0.05	0.688	<0.05	0.850	<0.05	0.146	<0.05
	<i>GS</i>	0.205	<0.05	0.043	<0.05	0.730	<0.05	0.825	<0.05	0.165	<0.05

Table 12: Results of the Vargha and Delaney statistics and the Mann–Whitney U test ($Jerk_{Reward}$) - RQ1

<i>DeepQTest</i> vs. (<i>RS</i> , <i>GS</i>)		<i>TTC</i>		<i>DTO</i>		<i>Jerk</i>		<i>#Collision</i>		<i>CollisionTime</i>	
		\hat{A}_{12}	<i>p</i>	\hat{A}_{12}	<i>p</i>	\hat{A}_{12}	<i>p</i>	\hat{A}_{12}	<i>p</i>	\hat{A}_{12}	<i>p</i>
<i>DeepQTest_{Jerk_{RD}}</i>											
<i>R1</i>	<i>RS</i>	0.618	0.208	0.338	0.081	0.682	<0.05	0.675	<0.05	0.315	<0.05
	<i>GS</i>	0.623	0.190	0.422	0.409	0.595	0.310	0.650	0.058	0.354	0.076
<i>R2</i>	<i>RS</i>	0.405	0.182	0.470	0.756	0.432	0.473	0.750	<0.05	0.244	<0.05
	<i>GS</i>	0.263	<0.05	0.472	0.776	0.422	0.409	0.825	<0.05	0.136	<0.05
<i>R3</i>	<i>RS</i>	0.160	<0.05	0.610	0.239	0.390	0.239	0.575	0.356	0.420	0.356
	<i>GS</i>	0.152	<0.05	0.578	0.409	0.405	0.310	0.650	0.058	0.335	<0.05
<i>R4</i>	<i>RS</i>	0.290	<0.05	0.228	<0.05	0.855	<0.05	0.800	<0.05	0.190	<0.05
	<i>GS</i>	0.180	<0.05	0.180	<0.05	0.815	<0.05	0.775	<0.05	0.229	<0.05
<i>DeepQTest_{Jerk_{RN}}</i>											
<i>R1</i>	<i>RS</i>	0.290	<0.05	0.435	0.490	0.782	<0.05	0.675	<0.05	0.360	0.104
	<i>GS</i>	0.225	<0.05	0.340	0.086	0.782	<0.05	0.725	<0.05	0.274	<0.05
<i>R2</i>	<i>RS</i>	0.177	<0.05	0.535	0.715	0.547	0.617	0.675	<0.05	0.286	<0.05
	<i>GS</i>	0.263	<0.05	0.512	0.903	0.560	0.525	0.700	<0.05	0.282	<0.05
<i>R3</i>	<i>RS</i>	0.280	<0.05	0.738x	<0.05	0.487	0.903	0.600	0.196	0.389	0.162
	<i>GS</i>	0.255	<0.05	0.642	0.126	0.510	0.925	0.550	0.534	0.424	0.359
<i>R4</i>	<i>RS</i>	0.152	<0.05	0.275	<0.05	0.690	<0.05	0.700	<0.05	0.304	<0.05
	<i>GS</i>	0.145	<0.05	0.215	<0.05	0.770	<0.05	0.775	<0.05	0.210	<0.05
<i>DeepQTest_{Jerk_{SD}}</i>											
<i>R1</i>	<i>RS</i>	0.237	<0.05	0.427	0.441	0.650	0.107	0.675	<0.05	0.273	<0.05
	<i>GS</i>	0.253	<0.05	0.502	0.989	0.568	0.473	0.700	<0.05	0.271	<0.05
<i>R2</i>	<i>RS</i>	0.273	<0.05	0.360	0.133	0.585	0.365	0.725	<0.05	0.240	<0.05
	<i>GS</i>	0.292	<0.05	0.482	0.860	0.625	0.181	0.700	<0.05	0.300	<0.05
<i>R3</i>	<i>RS</i>	0.085	<0.05	0.603	0.273	0.682	<0.05	0.750	<0.05	0.239	<0.05
	<i>GS</i>	0.237	<0.05	0.485	0.882	0.593	0.323	0.700	<0.05	0.297	<0.05
<i>R4</i>	<i>RS</i>	0.365	0.074	0.145	<0.05	0.720	<0.05	0.825	<0.05	0.165	<0.05
	<i>GS</i>	0.325	<0.05	0.158	<0.05	0.734	<0.05	0.825	<0.05	0.171	<0.05
<i>DeepQTest_{Jerk_{SN}}</i>											
<i>R1</i>	<i>RS</i>	0.445	0.561	0.393	0.250	0.680	0.053	0.625	0.110	0.390	0.176
	<i>GS</i>	0.365	0.148	0.557	0.543	0.593	0.323	0.650	0.051	0.333	<0.05
<i>R2</i>	<i>RS</i>	0.223	<0.05	0.485	0.882	0.695	<0.05	0.725	<0.05	0.297	<0.05
	<i>GS</i>	0.235	<0.05	0.455	0.636	0.660	0.086	0.700	<0.05	0.270	<0.05
<i>R3</i>	<i>RS</i>	0.110	<0.05	0.610	0.239	0.698	<0.05	0.750	<0.05	0.235	<0.05
	<i>GS</i>	0.182	<0.05	0.795x	<0.05	0.682	<0.05	0.625	0.118	0.366	0.135
<i>R4</i>	<i>RS</i>	0.355	<0.05	0.235	<0.05	0.647	0.114	0.825	<0.05	0.181	<0.05
	<i>GS</i>	0.320	<0.05	0.215	<0.05	0.650	0.107	0.825	<0.05	0.190	<0.05

Table 13: Results of the Vargha and Delaney statistics and the Mann–Whitney U test - RQ2

Reward Comparison			<i>TTC</i>		<i>DTO</i>		<i>Jerk</i>		#Collision		<i>CollisionTime</i>		<i>Div_{API}</i>		<i>Div_{Scenario}</i>	
			\hat{A}_{12}	<i>p</i>	\hat{A}_{12}	<i>p</i>	\hat{A}_{12}	<i>p</i>	\hat{A}_{12}	<i>p</i>	\hat{A}_{12}	<i>p</i>	\hat{A}_{12}	<i>p</i>	\hat{A}_{12}	<i>p</i>
<i>RD</i>																
<i>R1</i>	<i>DeepQTest_{TTC}</i>	<i>DeepQTest_{DTO}</i>	0.495	0.833	0.838×	<0.05	0.695	<0.05	0.525	0.722	0.496	0.978	0.551	0.583	0.521	0.828
		<i>DeepQTest_{Jerk}</i>	0.133	<0.05	0.250	<0.05	0.695	<0.05	0.625	0.099	0.364	0.134	0.338	0.079	0.334	0.073
<i>R2</i>	<i>DeepQTest_{DTO}</i>	<i>DeepQTest_{Jerk}</i>	0.128	<0.05	0.100	<0.05	0.542	0.655	0.600	0.196	0.354	0.108	0.276×	<0.05	0.302×	<0.05
		<i>DeepQTest_{DTO}</i>	0.125	<0.05	0.850×	<0.05	0.693	<0.05	0.425	0.225	0.535	0.692	0.514	0.884	0.492	0.946
<i>R3</i>	<i>DeepQTest_{TTC}</i>	<i>DeepQTest_{Jerk}</i>	0.217	<0.05	0.323	0.056	0.710	<0.05	0.475	0.722	0.459	0.650	0.460	0.662	0.445	0.560
		<i>DeepQTest_{Jerk}</i>	0.440	0.704	0.170	<0.05	0.552	0.579	0.550	0.394	0.453	0.604	0.471	0.758	0.476	0.807
<i>R4</i>	<i>DeepQTest_{DTO}</i>	<i>DeepQTest_{Jerk}</i>	0.458	0.640	0.855×	<0.05	0.522	0.818	0.550	0.534	0.471	0.756	0.565	0.484	0.547	0.421
		<i>DeepQTest_{Jerk}</i>	0.278	<0.05	0.113	<0.05	0.562	0.507	0.550	0.534	0.386	0.207	0.393	0.244	0.422	0.407
<i>R1</i>	<i>DeepQTest_{DTO}</i>	<i>DeepQTest_{Jerk}</i>	0.347	<0.05	0.055	<0.05	0.545	0.636	0.500	1.000	0.431	0.441	0.329	0.063	0.371	0.085
		<i>DeepQTest_{DTO}</i>	0.158	<0.05	0.868×	<0.05	0.578	0.409	0.600	0.154	0.461	0.678	0.499	1.000	0.284×	<0.05
<i>R2</i>	<i>DeepQTest_{TTC}</i>	<i>DeepQTest_{Jerk}</i>	0.122	<0.05	0.188	<0.05	0.583	0.379	0.600	0.154	0.378	0.183	0.407	0.318	0.296×	<0.05
		<i>DeepQTest_{Jerk}</i>	0.420	0.113	0.100	<0.05	0.530	0.756	0.500	1.000	0.419	0.373	0.420	0.390	0.454	0.625
<i>RN</i>																
<i>R1</i>	<i>DeepQTest_{TTC}</i>	<i>DeepQTest_{DTO}</i>	0.525	0.584	0.880×	<0.05	0.620	0.199	0.475	0.696	0.667	0.068	0.703	<0.05	0.686	<0.05
		<i>DeepQTest_{Jerk}</i>	0.188	<0.05	0.295	<0.05	0.578	0.409	0.575	0.302	0.396	0.258	0.396	0.263	0.380	0.197
<i>R2</i>	<i>DeepQTest_{DTO}</i>	<i>DeepQTest_{Jerk}</i>	0.290	<0.05	0.117	<0.05	0.455	0.636	0.600	0.154	0.264	<0.05	0.255×	<0.05	0.231×	<0.05
		<i>DeepQTest_{DTO}</i>	0.170	<0.05	0.855×	<0.05	0.757	<0.05	0.550	0.447	0.476	0.797	0.527	0.765	0.540	0.640
<i>R3</i>	<i>DeepQTest_{TTC}</i>	<i>DeepQTest_{Jerk}</i>	0.225	<0.05	0.145	<0.05	0.685	<0.05	0.650	<0.05	0.295	<0.05	0.320×	<0.05	0.338×	<0.05
		<i>DeepQTest_{Jerk}</i>	0.443	0.521	0.048	<0.05	0.445	0.561	0.600	0.196	0.333	0.060	0.292×	<0.05	0.352	0.054
<i>R4</i>	<i>DeepQTest_{DTO}</i>	<i>DeepQTest_{Jerk}</i>	0.378	0.189	0.820×	<0.05	0.472	0.776	0.425	0.302	0.547	0.603	0.565	0.476	0.501	1.000
		<i>DeepQTest_{DTO}</i>	0.168	<0.05	0.072	<0.05	0.588	0.351	0.600	0.215	0.352	0.094	0.443	0.539	0.326	0.061
<i>R1</i>	<i>DeepQTest_{TTC}</i>	<i>DeepQTest_{Jerk}</i>	0.307	<0.05	0.007	<0.05	0.650	0.107	0.675	<0.05	0.307	<0.05	0.379	0.189	0.241×	<0.05
		<i>DeepQTest_{Jerk}</i>	0.233	<0.05	0.880×	<0.05	0.562	0.507	0.450	0.447	0.613	0.219	0.664	0.074	0.453	0.811
<i>R2</i>	<i>DeepQTest_{DTO}</i>	<i>DeepQTest_{Jerk}</i>	0.335	0.076	0.177	<0.05	0.502	0.989	0.575	0.325	0.465	0.708	0.509	0.935	0.431	0.464
		<i>DeepQTest_{Jerk}</i>	0.652	0.514	0.072	<0.05	0.475	0.797	0.625	0.083	0.343	0.085	0.331	0.067	0.459	0.464
<i>SD</i>																
<i>R1</i>	<i>DeepQTest_{TTC}</i>	<i>DeepQTest_{DTO}</i>	0.512	0.903	0.912×	<0.05	0.675	0.060	0.550	0.482	0.549	0.602	0.603	0.269	0.544	0.645
		<i>DeepQTest_{Jerk}</i>	0.260	<0.05	0.245	<0.05	0.823	<0.05	0.625	0.099	0.431	0.453	0.500	1.000	0.361	0.136
<i>R2</i>	<i>DeepQTest_{DTO}</i>	<i>DeepQTest_{Jerk}</i>	0.270	<0.05	0.050	<0.05	0.698	<0.05	0.575	0.341	0.383	0.194	0.390	0.234	0.371	0.166
		<i>DeepQTest_{DTO}</i>	0.087	<0.05	0.865×	<0.05	0.760	<0.05	0.450	0.394	0.568	0.466	0.550	0.592	0.690	0.103
<i>R3</i>	<i>DeepQTest_{TTC}</i>	<i>DeepQTest_{Jerk}</i>	0.113	<0.05	0.147	<0.05	0.642	0.126	0.600	0.178	0.331	0.065	0.341	0.087	0.534	0.860
		<i>DeepQTest_{Jerk}</i>	0.345	0.337	0.100	<0.05	0.328	0.064	0.650	<0.05	0.259	<0.05	0.295×	<0.05	0.302×	<0.05
<i>R4</i>	<i>DeepQTest_{DTO}</i>	<i>DeepQTest_{Jerk}</i>	0.522	0.603	0.703×	<0.05	0.492	0.946	0.550	0.394	0.466	0.718	0.506	0.955	0.480	0.966
		<i>DeepQTest_{DTO}</i>	0.240	<0.05	0.048	<0.05	0.510	0.925	0.625	0.064	0.274	<0.05	0.285×	<0.05	0.256×	<0.05
<i>R1</i>	<i>DeepQTest_{TTC}</i>	<i>DeepQTest_{Jerk}</i>	0.275	<0.05	0.040	<0.05	0.502	0.989	0.575	0.302	0.330	0.063	0.328	0.061	0.338×	<0.05
		<i>DeepQTest_{Jerk}</i>	0.205	<0.05	0.885×	<0.05	0.605	0.262	0.550	0.447	0.551	0.571	0.552	0.563	0.329	0.065
<i>R2</i>	<i>DeepQTest_{DTO}</i>	<i>DeepQTest_{Jerk}</i>	0.120	<0.05	0.240	<0.05	0.613	0.229	0.575	0.270	0.346	0.094	0.364	0.140	0.300×	<0.05
		<i>DeepQTest_{Jerk}</i>	0.450	0.386	0.092	<0.05	0.535	0.715	0.525	0.740	0.321	<0.05	0.334	0.069	0.431	0.464
<i>SN</i>																
<i>R1</i>	<i>DeepQTest_{TTC}</i>	<i>DeepQTest_{DTO}</i>	0.323	0.056	0.815×	<0.05	0.522	0.818	0.575	0.270	0.430	0.449	0.441	0.529	0.406	0.315
		<i>DeepQTest_{Jerk}</i>	0.152	<0.05	0.180	<0.05	0.630	0.164	0.675	<0.05	0.250	<0.05	0.251×	<0.05	0.273×	<0.05
<i>R2</i>	<i>DeepQTest_{DTO}</i>	<i>DeepQTest_{Jerk}</i>	0.335	0.076	0.055	<0.05	0.713	<0.05	0.600	0.208	0.380	0.183	0.417	0.378	0.479	0.828
		<i>DeepQTest_{DTO}</i>	0.168	<0.05	0.848×	<0.05	0.790	<0.05	0.500	1.000	0.646	0.105	0.626	0.161	0.650	0.106
<i>R3</i>	<i>DeepQTest_{TTC}</i>	<i>DeepQTest_{Jerk}</i>	0.080	<0.05	0.135	<0.05	0.580	0.394	0.625	0.083	0.326	0.058	0.318×	<0.05	0.458	0.654
		<i>DeepQTest_{Jerk}</i>	0.390	0.133	0.077	<0.05	0.235×	<0.05	0.625	0.083	0.239	<0.05	0.261×	<0.05	0.302×	<0.05
<i>R4</i>	<i>DeepQTest_{DTO}</i>	<i>DeepQTest_{Jerk}</i>	0.688×	<0.05	0.750×	<0.05	0.640	0.133	0.500	1.000	0.499	1.000	0.468	0.729	0.390	0.237
		<i>DeepQTest_{DTO}</i>	0.325	0.060	0.010	<0.05	0.500	1.000	0.550	0.482	0.383	0.202	0.321	0.053	0.155×	<0.05
<i>R1</i>	<i>DeepQTest_{TTC}</i>	<i>DeepQTest_{Jerk}</i>	0.287	<0.05	0.005	<0.05	0.323	0.056	0.550	0.482	0.372	0.165	0.356	0.120	0.292×	<0.05
		<i>DeepQTest_{Jerk}</i>	0.355	0.273	0.895×	<0.05	0.552	0.579	0.500	1.000	0.574	0.417	0.576	0.403	0.416	0.371
<i>R2</i>	<i>DeepQTest_{DTO}</i>	<i>DeepQTest_{Jerk}</i>	0.198	<0.05	0.405	0.310	0.583	0.379	0.550	0.482	0.395	0.255	0.393	0.245	0.315×	<0.05
		<i>DeepQTest_{Jerk}</i>	0.347	0.064	0.098	<0.05	0.542	0.655	0.550	0.482	0.335	0.071	0.333	0.067	0.341	0.087